Clinicians' Guides to Radionuclide Hybrid Imaging · PET/CT
Series Editors: Jamshed B. Bomanji · Gopinath Gnanasegaran
Stefano Fanti · Homer A. Macapinlac

James R. Ballinger

PET Radiopharmaceuticals

Chemical, Biological, and Clinical Data

BNMS
BRITISH NUCLEAR MEDICINE SOCIETY

Springer

Clinicians' Guides to Radionuclide Hybrid Imaging

PET/CT

Series Editors
Jamshed B. Bomanji, Nuclear Medicine
University College Hospital
London, UK

Gopinath Gnanasegaran, Department of Nuclear Medicine
Royal Free London NHS Foundation Trust
London, UK

Stefano Fanti, Deptartment of Nuclear Medicine
Policlinico S.Orsola-Malpighi
Bologna, Bologna, Italy

Homer A. Macapinlac, Department of Nuclear Medicine
The University of Texas MD Anderson Cancer Center
Houston, TX, USA

Hybrid imaging with PET/CT and SPECT/CT provides high-quality information on function and structure, thereby permitting accurate localization, characterization, and diagnosis. There is extensive evidence to support the value of PET/CT, which has made a significant impact on oncological imaging and the management of patients with cancer. The evidence in favor of SPECT/CT, especially for orthopaedic indications, is evolving and increasing. This pocket book series on hybrid imaging (PET/CT and SPECT/CT) is specifically aimed at referring clinicians, nuclear medicine/radiology physicians, radiographers/technologists, and nurses who routinely work in nuclear medicine and participate in multidisciplinary meetings. The series will include 18 pocket books on PET/CT and 3 on SPECT/CT. Compiled under the auspices of the British Nuclear Medicine Society, the series is the joint work of many colleagues and professionals worldwide who share a common vision and purpose in promoting and supporting nuclear medicine as an important imaging specialty for the diagnosis and management of oncolo gical and non-oncological conditions.

The PET/CT pocket book series will be dedicated to some of the Society's recently departed peers, including Prof Ignac Fogelman, Dr Muriel Buxton-Thomas and Prof Ajit K Padhy

James R. Ballinger

PET Radiopharmaceuticals

Chemical, Biological, and Clinical Data

Springer

BNMS
BRITISH NUCLEAR MEDICINE SOCIETY

James R. Ballinger
School of Biomedical Engineering and Imaging Sciences
King's College London
London, UK

ISSN 2367-2439 ISSN 2367-2447 (electronic)
Clinicians' Guides to Radionuclide Hybrid Imaging - PET/CT
ISBN 978-3-031-10270-7 ISBN 978-3-031-10271-4 (eBook)
https://doi.org/10.1007/978-3-031-10271-4

This Springer imprint is published by the registered company Springer Nature Switzerland AG
The registered company address is: Gewerbestrasse 11, 6330 Cham, Switzerland

Acknowledgement

The author wishes to express his sincere thanks to Dr Gopinath Gnanasegaran, Royal Free Hospital, London, for his considerable assistance in the preparation of this book.

Introduction

Nuclear medicine is dependent on the availability of radiopharmaceuticals. The remarkable expansion of clinical PET over the past 20 years has occurred despite the challenges posed by the 110-min half-life of fluorine-18, the most widely used radionuclide. However, in much of the world there are now networks for production and distribution of PET radiopharmaceuticals.

Initially, clinical PET was based almost exclusively on one tracer, ^{18}F-fluorodeoxyglucose, FDG, an analogue of glucose. It is a truly remarkable molecule, initially developed to study neurophysiology, then myocardial metabolism, before its role in characterising tumours led to its acceptance in oncology. It has become the standard of care in a range of cancers, important in radiation treatment planning, and included in many clinical trials of new therapies.

But FDG can't do everything. This book brings together basic information about a range of alternative tracers used in oncology, cardiology, and neurology. Radionuclides other than ^{18}F are gradually becoming more widely used. Their properties are summarised in Table 1.

The production of a radiopharmaceutical involves a series of steps, each with its own challenges: working against the half-life of the radionuclide, safe handling of radioactive sources, and producing a drug suitable for intravenous administration to patients.

The first step is production of the radionuclide, most often in a cyclotron though there are other possibilities as outlined in Table 1. The radionuclide must then be

Table 1: Properties of selected positron emitting radionuclides

Radionuclide	Half- life	Positron energy (max, MeV)	Other emissions	Means of production
Carbon-11	20.4 min	0.98	None	Cyclotron
Nitrogen-13	9.97 min	1.19	None	Cyclotron
Oxygen-15	2.03 min	1.73	None	Cyclotron
Fluorine-18	110 min	0.63	None	Cyclotron
Copper-62	9.7 min	2.93	None	Generator
Copper-64	12.7 h	0.65	β^-, γ	Cyclotron
Gallium-68	68.3 min	1.90	None	Generator, cyclotron
Rubidium-82	1.25 min	3.18	γ	Generator
Zirconium-89	78.4 h	0.90	γ	Cyclotron
Iodine-124	100.3 h	1.53, 2.14	β^-, γ	Cyclotron

recovered from the irradiated target (solid, liquid, or gas) and transformed into a chemical and physical state suitable for the subsequent labelling reaction.

The radionuclide must then be attached to a precursor in order to produce the radiopharmaceutical. The efficiencies of these labelling reactions vary widely, and often the physical half-life of the radionuclide limits the duration of the reaction: after a certain time, there are diminishing returns as the label is decaying faster than the product is being produced. Following the labelling reaction, there may need to be a removal of protecting groups which ensured that the label attached at the correct position on the molecule. There is then a purification step to remove undesired reactants and by-products. Sometimes, this is a simple cartridge procedure, but it may involve high-pressure liquid chromatography (HPLC) and collection of the desired peak as it elutes. Finally, the collected fraction must be formulated and sterilised by membrane filtration.

Once the radiopharmaceutical has been produced, its quality must be checked against a variety of parameters. A pre-determined minimum set of tests must be completed before the radiopharmaceutical is released for use. Others are completed later; for example, sterility testing is not possible within the short period of time determined by the half-life of the radionuclide.

All in all, a complex series of operations, but with automated and validated processes it is practical to perform on a daily basis. Despite these challenges, PET radiopharmaceuticals have an impressive safety record.

At the time of writing, kit procedures for preparation of ^{68}Ga-labelled tracers are becoming available and their use with generator-produced ^{68}Ga may allow local preparation of tracers, but the impact of this remains to be seen.

Contents

Part VI Cardiology—Other Agents

Part VII Neurology—^{18}F-Labelled Agents

Part I

Oncology—^{18}F-Labelled Agents

^{18}F-Fluorodeoxyglucose (FDG)

Contents

Chemical name and alternative names	Chemical structure
2-[^{18}F]fluoro-2-deoxy-D-glucose; 2-deoxy-2-fluoro-D-glucose; fludeoxyglucose	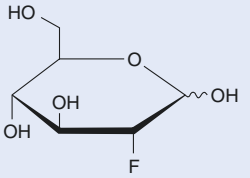

Route of Synthesis

Nucleophilic attack by ^{18}F-fluoride on mannose triflate, followed by base catalysed hydrolysis of acetyl protecting groups, purification by passage through alumina, C-18, and cation exchange solid phase extraction cartridges, and sterilisation by membrane filtration (Hamacher et al. 1986).

Normal Biodistribution and Excretion (Fig. 1)

Taken up by GLUT-1 glucose transporter and phosphorylated by hexokinase to FDG-6-phosphate. There is no further metabolism, and in most tissues there is negligible dephosphorylation. Avid uptake in brain (~7% of injected dose) and heart. Excreted via kidneys into bladder, with ~2% excreted within 2 h. Variable accumulation in muscle.

Activity Administered

400 MBq for tumour, inflammation, or myocardial imaging.

250 MBq for brain imaging in dementia or epilepsy.

J. R. Ballinger, *PET Radiopharmaceuticals*, Clinicians' Guides to Radionuclide Hybrid Imaging, https://doi.org/10.1007/978-3-031-10271-4_1

Radiation Dosimetry

Effective dose equivalent (mSv/MBq): 0.019 (8 mSv/400 MBq).

Organ doses (mGy/MBq): bladder wall, 0.16; heart, 0.062; brain, 0.028; kidneys, 0.021.

Patient Preparation

Patients should be well hydrated. For tumour imaging, blood glucose level should be <7 mmol/L. For myocardial imaging, patient should receive an oral glucose load of 50 g 1 h before injection of FDG. Patients should be rested, immobile, and kept warm during uptake period following injection in order to minimise accumulation in muscles and brown fat.

Clinical Utility

Diagnosis, staging, monitoring of therapeutic response, and evaluation of suspected recurrences in a variety of cancers. Evaluation of myocardial viability. Diagnosis of infection and/or inflammation. Evaluation of dementia. Identification of epileptogenic foci in presurgical evaluation of temporal lobe epilepsy (Dorbala et al. 2013; Boellaard et al. 2015).

Example Image

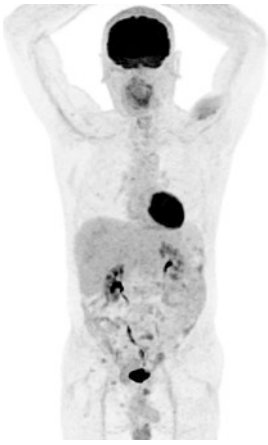

Fig. 1 Normal biodistribution of ^{18}F-FDG. Maximum intensity projection, anterior

Further Reading

Boellaard R, Delgado-Bolton R, Oyen WJ, et al. FDG PET/CT: EANM procedure guidelines for tumour imaging: version 2.0. Eur J Nucl Med Mol Imaging. 2015;42:328–54.

Dorbala S, Di Carli MF, Delbeke D, et al. SNMMI/ASNC/SCCT guideline for cardiac SPECT/CT and PET/CT 1.0. J Nucl Med. 2013;54:1485–507.

Hamacher K, Coenen HH, Stöcklin G. Efficient stereospecific synthesis of no-carrier-added 2-[^{18}F]fluoro-2-deoxy-D-glucose using amino-polyether supported nucleophilic substitution. J Nucl Med. 1986;27:235–8.

Sodium ^{18}F-Fluoride (NaF)

Contents

Chemical name and alternative names	Chemical structure
NaF	$Na^+ F^-$

Route of Synthesis

Directly from cyclotron irradiation of ^{18}O-water. Trapped on anion exchange cartridge and eluted with saline.

Normal Biodistribution and Excretion (Fig. 1)

Following intravenous administration, about 50% of the ^{18}F-fluoride is rapidly taken up by the skeleton where it remains during the time period of its radioactive decay. The remainder of the ^{18}F-fluoride is distributed into the extracellular fluid and eliminated by renal excretion within a few hours.

Activity Administered

370 MBq (100–400 MBq).

Radiation Dosimetry

Effective dose equivalent (mSv/MBq): 0.024 (9 mSv/370 MBq).

Organ doses (mGy/MBq): bladder, 0.22; bone surfaces, 0.04; red marrow, 0.04; kidneys, 0.02; uterus, 0.02.

Patient Preparation

Patients should be well hydrated before the start of the examination and urged to void as often as possible during the first hours after the study in order to reduce radiation dose.

J. R. Ballinger, *PET Radiopharmaceuticals*, Clinicians' Guides to Radionuclide Hybrid Imaging, https://doi.org/10.1007/978-3-031-10271-4_2

Clinical Utility

Sodium ^{18}F-fluoride PET is indicated for functional imaging in diseases where abnormally altered osteogenic activity is the diagnostic target. The following indications have been particularly documented: detection and localisation of bone metastases in case of cancer in adults; as an aid in the evaluation of back pain of ambiguous origin in adults, when conventional imaging modalities are not conclusive; as an aid in the detection of the presence of bone lesions related to suspected child abuse (Grant et al. 2008; Beheshti et al. 2009; Segall et al. 2010).

Example Image

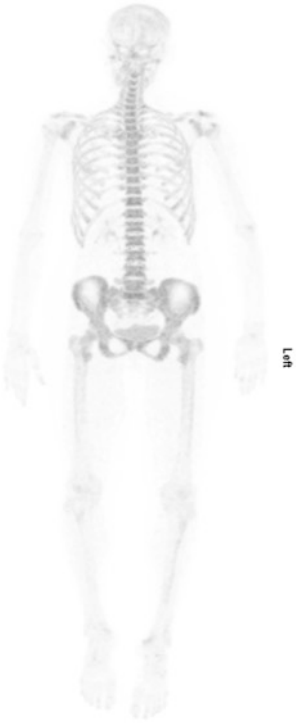

Fig. 1 Normal biodistribution of ^{18}F-fluoride. Maximum intensity projection, anterior

Further Reading

Beheshti M, Langsteger W, Fogelman I. Prostate cancer: role of SPECT and PET in imaging bone metastases. Semin Nucl Med. 2009;39:396–407.

Grant FD, Fahey FH, Packard AB, et al. Skeletal PET with ^{18}F-fluoride: applying new technology to an old tracer. J Nucl Med. 2008;49:68–78.

Segall G, Delbeke D, Stabin MG, et al. SNM practice guideline for sodium ^{18}F-fluoride PET/CT bone scans 1.0. J Nucl Med. 2010;51:1813–20.

^{18}F-Fluorothymidine (FLT)

Contents

Chemical name and alternative names	Chemical Structure
3′-fluoro-L-thymidine; 3′-deoxy-3′-fluorothymidine; alovudine	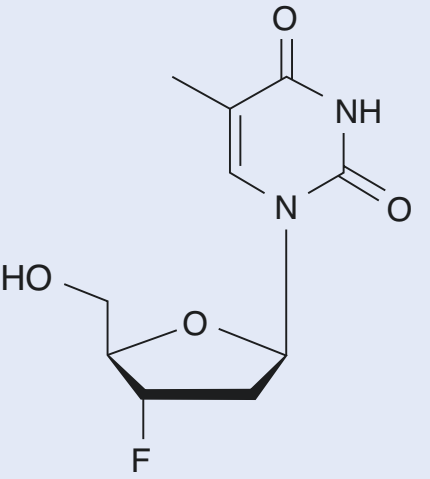

Route of Synthesis

Nucleophilic attack by ^{18}F-fluoride on an activated precursor, followed by hydrolysis of protecting groups and purification. Purification may be performed by HPLC or by solid phase extraction cartridge.

J. R. Ballinger, *PET Radiopharmaceuticals*, Clinicians' Guides to Radionuclide Hybrid Imaging, https://doi.org/10.1007/978-3-031-10271-4_3

Normal Biodistribution and Excretion

Distributes rapidly throughout the body. Retained in liver and bone marrow. Does not cross the blood–brain barrier. Clears rapidly from the blood. Primarily renal excretion with 30–50% of the dose recovered in urine in 2 h.

Activity Administered

185 MBq or 3 MBq/kg.

Radiation Dosimetry

Effective dose equivalent (mSv/MBq): 0.028 (5 mSv/185 MBq).

Organ doses (mGy/MBq): urinary bladder wall, 0.18 (6 h void); liver, 0.05; kidneys, 0.04; bone marrow, 0.03 (Vesselle et al. 2003).

Patient Preparation

Patient preparation is not standardised yet.

Clinical Utility

Proliferating tissues, primarily in cancer. Thymidine kinase I (TK1) activity is thought to be proportional to cellular proliferation and DNA synthesis by the salvage pathway. FLT is phosphorylated by TK1 and trapped in proliferating cells but not incorporated into DNA. Imaging of tumour proliferation. Prediction of therapy response, particularly in brain, lung, and breast cancers (Chalkidou et al. 2012; Soloviev et al. 2012; Bollineni et al. 2016).

Further Reading

Bollineni VR, Kramer GM, Jansma EP, et al. A systematic review on [^{18}F]FLT-PET uptake as a measure of treatment response in cancer patients. Eur J Cancer. 2016;55:81–97.

Chalkidou A, Landau DB, Odell EW, et al. Correlation between Ki-67 immunohistochemistry and ^{18}F-fluorothymidine uptake in patients with cancer: a systematic review and meta-analysis. Eur J Cancer. 2012;48:3499–513.

Soloviev D, Lewis D, Honess D, et al. [^{18}F]FLT: an imaging bio-marker of tumour proliferation for assessment of tumour response to treatment. Eur J Cancer. 2012;48:416–424.

Vesselle H, Grierson J, Peterson LM, et al. ^{18}F-Fluorothymidine radiation dosimetry in human PET imaging studies. J Nucl Med. 2003;44:1482–1488.

^{18}F-Fluoromethylcholine

Contents

Chemical name and alternative names	Chemical structure
Fluoromethyl-dimethyl-2-hydroxyethylammonium; fluorocholine; FCh; FCH; FMC; F-Choline	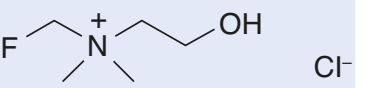

Route of Synthesis

Nucleophilic displacement by ^{18}F-fluoride on dibromomethane, followed by reaction with *N*,*N*-dimethylaminoethanol. The product is trapped on a cation exchange cartridge, washed with ethanol and water, and eluted with saline (DeGrado et al. 2001; Iwata et al. 2002).

Normal Biodistribution and Excretion (Fig. 1)

Rapid distribution and blood clearance with little change after 10 min. Highest uptake in kidneys, liver, and spleen. Less than 10% of dose excreted in urine.

Activity Administered

300 MBq or 4 MBq/kg.

Radiation Dosimetry

Effective dose equivalent (mSv/MBq): 0.02 (6 mSv/300 MBq).

Organ doses (mGy/MBq): kidneys, 0.08; liver, 0.06; spleen, 0.04; urinary bladder wall, 0.03 (DeGrado et al. 2002; Giussani et al. 2012).

J. R. Ballinger, *PET Radiopharmaceuticals*, Clinicians' Guides to Radionuclide Hybrid Imaging, https://doi.org/10.1007/978-3-031-10271-4_4

Patient Preparation

Patient preparation is not standardised yet.

Clinical Utility

Taken into cells by choline transporters, phosphorylated by choline kinase overexpressed in tumours and incorporated into membranes. Particularly useful in prostate cancer, in part because of relatively low urinary excretion, though more than ^{11}C-choline. Also in breast cancer and brain tumours (Mertens et al. 2010).

Example Image

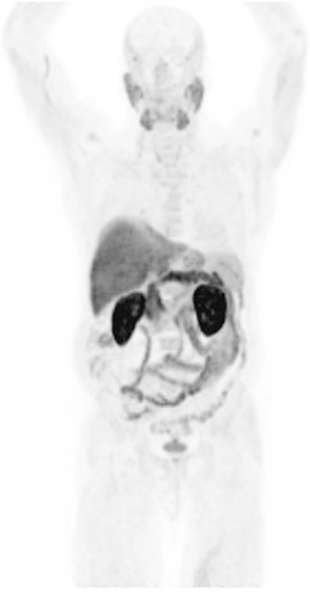

Fig. 1 Normal biodistribution of ^{18}F-fluoromethylcholine. Maximum intensity projection, anterior

Further Reading

DeGrado TR, Coleman RE, Wang S, et al. Synthesis and evaluation of ^{18}F-labeled choline as an oncologic tracer for positron emission tomography: initial findings in prostate cancer. Cancer Res. 2001;61:110–7.

DeGrado TR, Reiman RE, Price DT, et al. Pharmacokinetics and radiation dosimetry of ^{18}F-fluorocholine. J Nucl Med. 2002;43:92–6.

Giussani A, Janzen T, Uusijärvi-Lizana H, et al. A compartmental model for biokinetics and dosimetry of ^{18}F-choline in prostate cancer patients. J Nucl Med. 2012;53:985–93.

Iwata R, Pascali C, Bogni A, et al. [^{18}F]Fluoromethyl triflate, a novel and reactive [^{18}F]fluoromethylating agent: preparation and application to the on-column preparation of [^{18}F]fluorocholine. Appl Radiat Isot. 2002;57:347–352.

Mertens K, Slaets D, Lambert B, et al. PET with ^{18}F-fluorocholine-based tracers for tumour imaging: a review of the literature. Eur J Nucl Med Mol Imaging. 2010;37:2188–93.

^{18}F-Fluoroethylcholine (FECh)

Contents

Chemical name and alternative names	Chemical structure
2-Fluoroethyl-dimethyl-2-hydroxyethylammonium; FEtCh; FEC	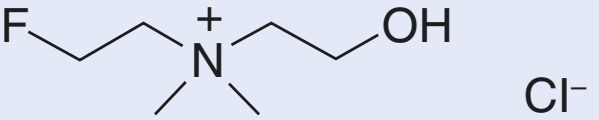

Route of Synthesis

Nucleophilic reaction between ^{18}F-fluoride and 1,2-ditosyloxy-ethane, followed by reaction with N,N-dimethylethanolamine. Product is trapped on a cation exchange cartridge, then eluted with saline (Hara et al. 2002; Schmaljohann et al. 2011).

Normal Biodistribution and Excretion

Similar to ^{18}F-fluoromethylcholine, except for greater extent of urinary excretion which may require catheterisation. Highest activity in urinary bladder, kidneys, and liver.

Activity Administered

300 MBq.

J. R. Ballinger, *PET Radiopharmaceuticals*, Clinicians' Guides to Radionuclide Hybrid Imaging, https://doi.org/10.1007/978-3-031-10271-4_5

Radiation Dosimetry

Effective dose equivalent (mSv/MBq): 0.035 (10 mSv/300 MBq).

Patient Preparation

Patients should be well hydrated to reduce urinary activity and allow better detectability of retroperitoneal and pelvic lesions.

Clinical Utility

See ^{18}F-fluoromethylcholine (Tilki et al. 2013; Hartenbach et al. 2014; Haroon et al. 2017).

Further Reading

Hara T, Kosaka N, Kishi H. Development of ^{18}F-fluoroethyl-choline for cancer imaging with PET: synthesis, biochemistry, and prostate cancer imaging. J Nucl Med. 2002;43:187–99.

Haroon A, Syed R, Endozo R, Allie R, et al. Spectrum of metastatic and nonmetastatic skeletal findings with dual-phase ^{18}F-FECH PET/CT in patients with biochemical relapse of prostate cancer. Nucl Med Commun. 2017;38:407–14.

Hartenbach M, Hartenbach S, Bechtloff W, et al. Combined PET/MRI improves diagnostic accuracy in patients with prostate cancer: a prospective diagnostic trial. Clin Cancer Res. 2014;20:3244–53.

Schmaljohann J, Schirrmacher E, Wängler B, et al. Fully automated SPE-based synthesis and purification of 2-[^{18}F]fluoroethyl-choline for human use. Nucl Med Biol. 2011;38:165–70.

Tilki D, Reich O, Graser A, et al. ^{18}F-Fluoroethylcholine PET/CT identifies lymph node metastasis in patients with prostate-specific antigen failure after radical prostatectomy but underestimates its extent. Eur Urol. 2013;63:792–796.

^{18}F-Fluoroethyltyrosine (FET)

Contents

Chemical name and alternative names	Chemical structure
O-(2-^{18}F-fluoroethyl)-L-tyrosine	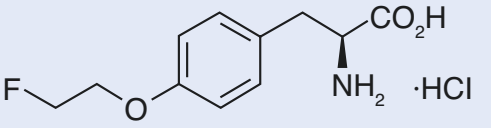

Route of Synthesis

Nucleophilic reaction between ^{18}F-fluoride and protected tosyl precursor, followed by hydrolysis of protecting group with trifluoroacetic acid and workup by solid phase extraction. Purified by HPLC using 2% ethanol in water as eluant; product fraction sterile filtered (Hamacher et al. 2002).

Normal Biodistribution and Excretion

Taken up by amino acid transport system L. Neither incorporated into protein nor metabolised. Activity clears rapidly from circulation. Cleared almost entirely via the kidneys (Pauleit et al. 2003).

Activity Administered

200 MBq.

J. R. Ballinger, *PET Radiopharmaceuticals*, Clinicians' Guides to Radionuclide Hybrid Imaging, https://doi.org/10.1007/978-3-031-10271-4_6

Radiation Dosimetry

Effective dose equivalent (mSv/MBq): 0.016 (3.2 mSv/200 MBq).
Organ doses (mGy/MBq): urinary bladder, 0.085; kidneys, 0.027.

Patient Preparation

No specific preparation.

Clinical Utility

Amino acid transport in tumours. Useful for grading of glioma (Weckesser et al. 2005; Langen et al. 2006; Albert et al. 2016).

Further Reading

Albert NL, Winkelmann I, Suchorska B, et al. Early static [18]F-FET-PET scans have a higher accuracy for glioma grading than the standard 20–40 min scans. Eur J Nucl Med Mol Imaging. 2016;43:1105–14.

Hamacher K, Coenen HH. Efficient routine production of the [18]F-labelled amino acid O-(2-[[18]F]fluoroethyl)-L-tyrosine. Appl Radiat Isot. 2002;57:853–6.

Langen KJ, Hamacher K, Weckesser M, et al. O-(2-[[18]F]fluoroethyl)-L-tyrosine: uptake mechanisms and clinical applications. Nucl Med Biol. 2006;33:287–94.

Pauleit D, Floeth F, Herzog H, et al. Whole-body distribution and dosimetry of O-(2-[[18]F]fluoroethyl)-L-tyrosine. Eur J Nucl Med Mol Imaging. 2003;30:519–24.

Weckesser M, Langen KJ, Rickert CH, et al. O-(2-[[18]F]fluoroethyl)-L-tyrosine PET in the clinical evaluation of primary brain tumours. Eur J Nucl Med Mol Imaging. 2005;32:422–9.

^{18}F-Fluoromisonidazole (FMISO)

Contents

Chemical name and alternative names	Chemical structure
1-Fluoro-3-(2-nitro-imidazol-1-yl)-propan-2-ol	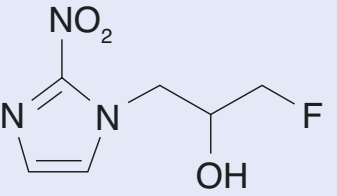

Route of Synthesis

Nucleophilic reaction of ^{18}F-fluoride with a tosylated precursor, followed by hydrolysis of protecting group and purification trapping on a solid phase extraction cartridge and elution with aqueous ethanol. Can be adapted to FDG synthesis module (Oh et al. 2005).

Normal Biodistribution and Excretion

Rapid clearance from circulation. Clearance through liver and kidneys, but only ~3% excreted in urine.

Activity Administered

300 MBq or 4 MBq/kg.

J. R. Ballinger, *PET Radiopharmaceuticals*, Clinicians' Guides to Radionuclide Hybrid Imaging, https://doi.org/10.1007/978-3-031-10271-4_7

Radiation Dosimetry

Effective dose equivalent (mSv/MBq): 0.013 (4 mSv/300 MBq).

Organ doses (mGy/MBq): urinary bladder wall, 0.02; other organs slightly lower (Graham et al. 1997).

Patient Preparation

No specific preparation.

Clinical Utility

Hypoxia imaging. Accumulates in hypoxic regions of tumours (hot spot imaging) by bioreductive process; clears from normoxic regions. Has shown utility in head and neck cancer, glioblastoma multiforme, and breast cancer (Lopci et al. 2014).

Further Reading

Graham MM, Peterson LM, Link JM, et al. Fluorine-18-fluoromisonidazole radiation dosimetry in imaging studies. J Nucl Med. 1997;38:1631–6.

Lopci E, Grassi I, Chiti A, et al. PET radiopharmaceuticals for imaging of tumor hypoxia: a review of the evidence. Am J Nucl Med Mol Imaging. 2014;4:365–84.

Oh SJ, Chi DY, Mosdzianowski C, et al. Fully automated synthesis of [^{18}F]fluoromisonidazole using a conventional [^{18}F]FDG module. Nucl Med Biol. 2005;32:899–905.

^{18}F-Fluoroazomycin Arabinoside (FAZA)

Contents

Chemical name and alternative names	Chemical structure
1-(5-fluoro-5-deoxy-alpha-D-arabinofuranosyl)-2-nitro-imidazole	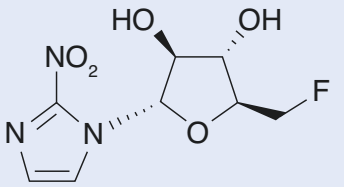

Route of Synthesis

Nucleophilic reaction between ^{18}F-fluoride and tosylated precursor, followed by hydrolysis of protecting groups and purification (Hayashi et al. 2011).

Normal Biodistribution and Excretion

Rapid distribution throughout the body. More rapid clearance from background than FMISO, resulting in higher target/background ratios. Hepatobiliary and renal excretion. At 2 h post injection, relative organ activities are: kidney > gallbladder > liver > tumour > muscle > bone > brain > lung (Savi et al. 2017).

Activity Administered

300 MBq.

J. R. Ballinger, *PET Radiopharmaceuticals*, Clinicians' Guides to Radionuclide Hybrid Imaging, https://doi.org/10.1007/978-3-031-10271-4_8

Radiation Dosimetry

Effective dose (mSv/MBq): 0.015 (4.5 mSv/300 MBq).

Organ doses (mGy/MBq): urinary bladder wall, 0.047; uterus, 0.020; heart wall, 0.018; kidneys, 0.017.

Patient Preparation

No specific preparation.

Clinical Utility

Hypoxia imaging. Promising preliminary results in head and neck squamous cell carcinoma, non-small cell lung carcinoma, cervical carcinoma, and glioma (Postema et al. 2009; Lopci et al. 2014; Halmos et al. 2014).

Further Reading

Halmos GB, Bruine de Bruin L, Langendijk JA, et al. Head and neck tumor hypoxia imaging by ^{18}F-fluoroazomycin-arabinoside (^{18}F-FAZA)-PET: a review. Clin Nucl Med. 2014;39:44–8.

Hayashi K, Furutsuka K, Takei M, et al. High-yield automated synthesis of [^{18}F]fluoroazomycin arabinoside ([^{18}F]FAZA) for hypoxia-specific tumor imaging. Appl Radiat Isot. 2011;69:1007–13.

Lopci E, Grassi I, Chiti A, et al. PET radiopharmaceuticals for imaging of tumor hypoxia: a review of the evidence. Am J Nucl Med Mol Imaging. 2014;4:365–84.

Postema EJ, McEwan AJ, Riauka TA, et al. Initial results of hypoxia imaging using 1-alpha-D:-(5-deoxy-5-[^{18}F]-fluoroarabinofuranosyl)-2-nitroimidazole (^{18}F-FAZA). Eur J Nucl Med Mol Imaging. 2009;36:1565–73.

Savi A, Incerti E, Fallanca F, et al. First evaluation of PET-based human biodistribution and dosimetry of ^{18}F-FAZA, a tracer for imaging tumor hypoxia. J Nucl Med. 2017;58:1224–9.

^{18}F-Fluoroerythronitroimidazole (FETNIM)

Contents

Chemical name and alternative names	Chemical structure
1-Fluoro-4-(2-nitro-1H-imidazol-1-yl)-, [R-(R*, S*)]-2,3-butanediol	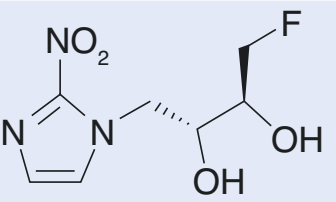

Route of Synthesis

Nucleophilic reaction between ^{18}F-fluoride and tosylated precursor, followed by hydrolysis of protecting group.

Normal Biodistribution and Excretion

Rapid clearance from blood and organs. About 50% of dose excreted in urine within 4 h. More hydrophilic than FMISO, thus background should clear more rapidly (Grönoroos et al. 2001).

J. R. Ballinger, *PET Radiopharmaceuticals*, Clinicians' Guides to Radionuclide Hybrid Imaging, https://doi.org/10.1007/978-3-031-10271-4_9

Activity Administered

370 MBq.

Radiation Dosimetry

Effective dose equivalent (mSv/MBq): 0.015 (6 mSv/370 MBq).
Organ doses (mGy/MBq): urinary bladder wall, 0.062 (Tolvanen et al. 2002).

Patient Preparation

No specific preparation.

Clinical Utility

Hypoxia imaging. Has been studied in head and neck, oesophageal, and lung cancer (Lethiö et al. 2004; Grönroos et al. 2014; Hu et al. 2020).

Further Reading

Grönroos T, Eskola O, Lethiö K, et al. Pharmacokinetics of [^{18}F]FETNIM, a potential hypoxia marker for PET. J Nucl Med. 2001;42:1397–404.

Grönroos TJ, Lehtiö K, Söderström KO, et al. Hypoxia, blood flow and metabolism in squamous-cell carcinoma of the head and neck: correlations between multiple immunohistochemical parameters and PET. BMC Cancer. 2014;14:876.

Hu M, Zhu Y, Mu D, et al. Correlation of hypoxia as measured by fluorine-18 fluoroerythronitroimidazole (^{18}F-FETNIM) PET/CT and overall survival in glioma patients. Eur J Nucl Med Mol Imaging. 2020;47:1427–34.

Lethiö K, Eskola O, Viljanen T, et al. Imaging perfusion and hypoxia with PET to predict radiotherapy response in head-and-neck cancer. Int J Radiat Oncol Biol Phys. 2004;59:971–82.

Tolvanen T, Lehtiö K, Kulmala J, et al. ^{18}F-Fluoroerythronitroimidazole radiation dosimetry in cancer studies. J Nucl Med. 2002;43:1674–1680.

^{18}F-HX4

Contents

Chemical name and alternative names	Chemical structure
3-[^{18}F]fluoro-2-(4-((2-nitro-1H-imidazol-1-yl) methyl)-1H-1,2,3-triazol-1-yl)propan-1-ol; Flortanidazole; (Siemens)	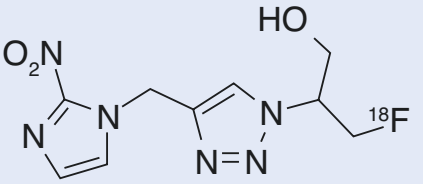

Route of Synthesis

Nucleophilic reaction between ^{18}F-fluoride and an activated precursor, followed by hydrolysis of protecting group, purification, and reformulation.

Normal Biodistribution and Excretion

Rapid clearance from blood and organs. About 45% of dose excreted in urine within 4 h. Background clearance is more rapid than FMISO which may allow earlier imaging (Doss et al. 2010).

Activity Administered

400 MBq.

J. R. Ballinger, *PET Radiopharmaceuticals*, Clinicians' Guides to Radionuclide Hybrid Imaging, https://doi.org/10.1007/978-3-031-10271-4_10

Radiation Dosimetry

Effective dose equivalent (mSv/MBq): 0.027 (10.8 mSv/400 MBq).
Organ doses (mGy/MBq): urinary bladder wall, 0.30 (Doss et al. 2010).

Patient Preparation

No specific preparation.

Clinical Utility

Hypoxia imaging. Has been studied in head and neck and primary and metastatic lung cancer (van Loon et al. 2010; Zegers et al. 2013, 2015, 2016; Sanduleanu et al. 2020).

Further Reading

Doss M, Zhang JJ, Bélanger MJ, et al. Biodistribution and radiation dosimetry of the hypoxia marker ^{18}F-HX4 in monkeys and humans determined by using whole-body PET/CT. Nucl Med Commun. 2010;31:1016–24.

Sanduleanu S, Wiel AM, Lieverse RI, et al. Hypoxia PET imaging with [^{18}F]-HX4-a promising next-generation tracer. Cancers (Basel). 2020;12:1322.

van Loon J, Janssen MH, Ollers M, et al. PET imaging of hypoxia using [^{18}F]HX4: a phase I trial. Eur J Nucl Med Mol Imaging. 2010;37:1663–8.

Zegers CM, Hoebers FJ, van Elmpt W, et al. Evaluation of tumour hypoxia during radiotherapy using [^{18}F]HX4 PET imaging and blood biomarkers in patients with head and neck cancer. Eur J Nucl Med Mol Imaging. 2016;43:2139–46.

Zegers CM, van Elmpt W, Szardenings K, et al. Repeatability of hypoxia PET imaging using [^{18}F]HX4 in lung and head and neck cancer patients: a prospective multicenter trial. Eur J Nucl Med Mol Imaging. 2015;42:1840–9.

Zegers CM, van Elmpt W, Wierts R, et al. Hypoxia imaging with [^{18}F]HX4 PET in NSCLC patients: defining optimal imaging parameters. Radiother Oncol. 2013;109:58–64.

^{18}F-Fluciclatide

Contents

Chemical name and alternative names	Chemical structure
AH111585	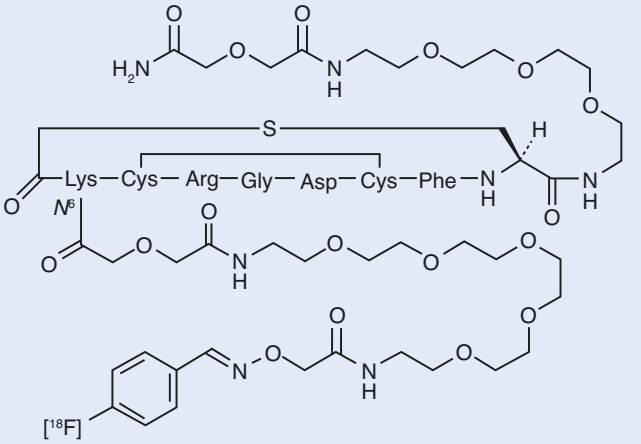

Route of Synthesis

Coupling of 4-^{18}F-fluorobenzaldehyde with aminooxy-functionalised precursor to form oxime.

J. R. Ballinger, *PET Radiopharmaceuticals*, Clinicians' Guides to Radionuclide Hybrid Imaging, https://doi.org/10.1007/978-3-031-10271-4_11

Normal Biodistribution and Excretion

Initial high uptake in liver, spleen, and heart wall followed by clearance. Excretion is 37% via kidneys and 20% via liver. Biological half-life in whole blood is 0.25 h (McParland et al. 2008).

Activity Administered

370 MBq.

Radiation Dosimetry

Effective dose equivalent (mSv/MBq): 0.026 (10 mSv/370 MBq).

Organ doses (mGy/MBq): urinary bladder wall, 0.12; kidneys, 0.10; cardiac wall 0.06 (McParland et al. 2008).

Patient Preparation

Patient preparation is not standardised yet.

Clinical Utility

Targets $\alpha_v\beta_3$ integrin for imaging angiogenesis. Has been shown to be taken up in breast cancer, melanoma, and renal tumours (Tomasi et al. 2011; Mena et al. 2014; Sharma et al. 2015, 2020).

Further Reading

McParland BJ, Miller MP, Spinks TJ, et al. The biodistribution and radiation dosimetry of the Arg-Gly-asp peptide ^{18}F-AH111585 in healthy volunteers. J Nucl Med. 2008;49:1664–7.

Mena E, Owenius R, Turkbey B, et al. [^{18}F]Fluciclatide in the in vivo evaluation of human melanoma and renal tumors expressing $\alpha_v\beta_3$ and $\alpha_v\beta_5$ integrins. Eur J Nucl Med Mol Imaging. 2014;41:1879–1888.

Sharma R, Kallur KG, Ryu JS, et al. Multicenter reproducibility of ^{18}F-fluciclatide PET imaging in subjects with solid tumors. J Nucl Med. 2015;56:1855–61.

Sharma R, Valls PO, Inglese M, et al. [^{18}F]Fluciclatide PET as a biomarker of response to combination therapy of pazopanib and paclitaxel in platinum-resistant/refractory ovarian cancer. Eur J Nucl Med Mol Imaging. 2020;47:1239–1251.

Tomasi G, Kenny L, Mauri F, et al. Quantification of receptor-ligand binding with [^{18}F]fluciclatide in metastatic breast cancer patients. Eur J Nucl Med Mol Imaging. 2011;38:2186–97.

^{18}F-Galacto-RGD

Contents

Chemical name, alternative names	Chemical structure
Cyclo [L-arginylglycyl-L-α-aspartyl-D-phenylalanyl-N6-[2,6-anhydro-7-deoxy-7-[[2-fluoro-1-oxopropyl] amino]-L-glycero-L-galacto-heptonoyl]-L-lysyl]	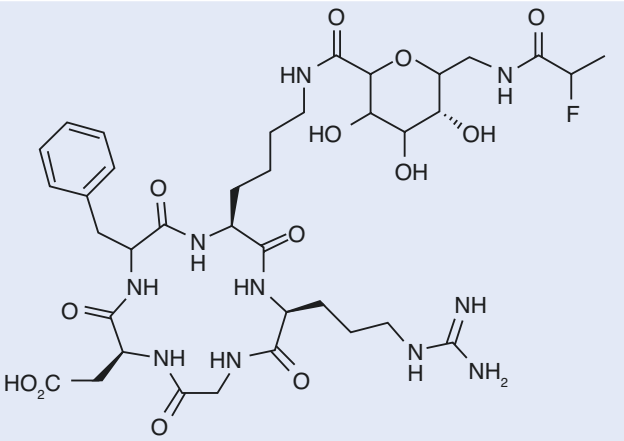

Route of Synthesis

Two-step synthesis from ^{18}F-fluoride with initial production of ^{18}F propionate prosthetic group then coupling to galacto-RGD (Haubner et al. 2004).

J. R. Ballinger, *PET Radiopharmaceuticals*, Clinicians' Guides to Radionuclide Hybrid Imaging, https://doi.org/10.1007/978-3-031-10271-4_12

Normal Biodistribution and Excretion

Rapid clearance from blood pool with primarily renal excretion. Low background activity in lungs and muscle.

Activity Administered

200 MBq.

Radiation Dosimetry

Effective dose equivalent (mSv/MBq): 0.019 (4 mSv/200 MBq).

Organ doses (mGy/MBq): bladder wall, 0.22; kidneys, 0.03; liver, 0.02 (Beer et al. 2006).

Patient Preparation

No specific preparation.

Clinical Utility

Imaging of angiogenesis. Has been evaluated in sarcoma, melanoma, renal cell cancer, head and neck, breast cancer, and glioblastoma multiforme. Detection of primary tumour is high, but lower detection rate for lymph nodes and distant metastases. Also taken up in some chronic inflammatory lesions (Beer et al. 2007; Haubner et al. 2014).

Further Reading

Beer AJ, Grosu AL, Carlsen J, et al. [^{18}F]Galacto-RGD positron emission tomography for imaging of alpha$_v$beta$_3$ expression on the neovasculature in patients with squamous cell carcinoma of the head and neck. Clin Cancer Res. 2007;13:6610–6.

Beer AJ, Haubner R, Wolf I, et al. PET-based human dosimetry of ^{18}F-galacto-RGD, a new radiotracer for imaging alpha$_v$ beta$_3$ expression. J Nucl Med. 2006;47:763–9.

Haubner R, Kuhnast B, Mang C, et al. [^{18}F]Galacto-RGD: synthesis, radiolabeling, metabolic stability, and radiation dose estimates. Bioconjug Chem. 2004;15:61–9.

Haubner R, Maschauer S, Prante O. PET radiopharmaceuticals for imaging integrin expression: tracers in clinical studies and recent developments. Biomed Res Int. 2014;2014:871609.

^{18}F-Fluciclovine (FACBC)

Contents

Chemical name and alternative names	Chemical structure
Anti-1-amino-3-^{18}F-fluorocyclobutane-1-carboxylic acid; FACBC; Axumin™ (Blue Earth Diagnostics)	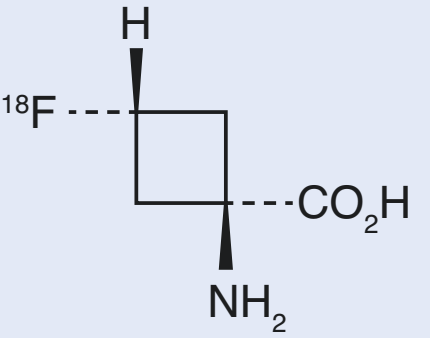

Route of Synthesis

Nucleophilic attack of ^{18}F-fluoride on triflate precursor, followed by deprotection with HCl and purification using solid phase extraction cartridges.

Normal Biodistribution and Excretion

Highest initial uptake in liver, bone marrow, and lung. Very little urinary or hepatobiliary excretion (~3% in urine over 4 h) (Sörensen et al. 2013).

J. R. Ballinger, *PET Radiopharmaceuticals*, Clinicians' Guides to Radionuclide Hybrid Imaging, https://doi.org/10.1007/978-3-031-10271-4_13

Activity Administered

370 MBq.

Radiation Dosimetry

Effective dose equivalent (mSv/MBq): 0.022 (8 mSv/370 MBq).

Organ doses (mGy/MBq): pancreas, 0.10; cardiac wall, 0.05; uterine wall, 0.04 (McParland et al. 2013).

Patient Preparation

Patients should avoid significant exercise for 1 day before imaging. Patients should not eat or drink for 4 h before imaging.

Clinical Utility

Amino acid transport in tumours. Particularly useful in prostate cancer because of lack of urinary activity (Nanni et al. 2016, 2020; Marcus et al. 2020).

Further Reading

Marcus C, Butler P, Bagrodia A, Cole S, et al. Fluorine-18-labeled fluciclovine PET/CT in primary and biochemical recurrent prostate cancer management. AJR Am J Roentgenol. 2020;215:267–76.

McParland BJ, Wall A, Johansson S, et al. The clinical safety, biodistribution and internal radiation dosimetry of [^{18}F]fluciclovine in healthy adult volunteers. Eur J Nucl Med Mol Imaging. 2013;40:1256–64.

Nanni C, Zanoni L, Bach-Gansmo T, et al. [^{18}F]Fluciclovine PET/CT: joint EANM and SNMMI procedure guideline for prostate cancer imaging–version 1.0. Eur J Nucl Med Mol Imaging. 2020;47:579–591.

Nanni C, Zanoni L, Pultrone C, et al. ^{18}F-FACBC (anti1-amino-3-^{18}F-fluorocyclobutane-1-carboxylic acid) versus ^{11}C-choline PET/CT in prostate cancer relapse: results of a prospective trial. Eur J Nucl Med Mol Imaging. 2016;43:1601–1610.

Sörensen J, Owenius R, Lax M, et al. Regional distribution and kinetics of [^{18}F]fluciclovine (anti-[^{18}F]FACBC), a tracer of amino acid transport, in subjects with primary prostate cancer. Eur J Nucl Med Mol Imaging. 2013;40:394–402.

^{18}F-ICMT11

Contents

Chemical name and alternative names	Chemical structure
^{18}F-(S)-1-((1-(2-fluoroethyl)-1H-[1,2,3]-triazol-4-yl)methyl)-5-(2(2,4-difluorophenoxymethyl)-pyrrolidine-1-sulfonyl)isatin	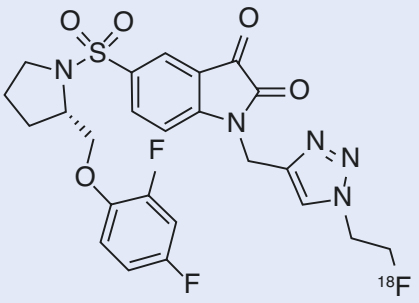

Route of Synthesis

Nucleophilic attack of ^{18}F-fluoride on tosylate precursor followed by HPLC purification and reformulation (Fortt et al. 2012).

Normal Biodistribution and Excretion

Rapid distribution with elimination via both kidneys and intestines. Liver activity clears over 3 h (Challapalli et al. 2013).

Activity Administered

370 MBq.

J. R. Ballinger, *PET Radiopharmaceuticals*, Clinicians' Guides to Radionuclide Hybrid Imaging, https://doi.org/10.1007/978-3-031-10271-4_14

Radiation Dosimetry

Effective dose equivalent (mSv/MBq): 0.025 (9 mSv/370 MBq).

Organ doses (mGy/MBq): gall bladder wall, 0.59; small intestine, 0.12; upper large intestinal wall, 0.08; urinary bladder wall, 0.07; liver, 0.07 (Challapalli et al. 2013).

Patient Preparation

Patient preparation is not standardised yet.

Clinical Utility

Detection of apoptosis as biomarker of response to chemotherapy or radiotherapy (Nguyen et al. 2012; Dubash et al. 2018; García-Argüello et al. 2020).

Further Reading

Challapalli A, Kenny LM, Hallett WA, et al. ^{18}F-ICMT-11, a caspase-3-specific PET tracer for apoptosis: biodistribution and radiation dosimetry. J Nucl Med. 2013;54:1551–1556.

Dubash SR, Merchant S, Heinzmann K, et al. Clinical translation of [^{18}F]ICMT-11 for measuring chemotherapy-induced caspase 3/7 activation in breast and lung cancer. Eur J Nucl Med Mol Imaging. 2018;45:2285–99.

Fortt R, Smith G, Awais RO, et al. Automated GMP synthesis of [^{18}F]ICMT-11 for in vivo imaging of caspase-3 activity. Nucl Med Biol. 2012;39:1000–5.

García-Argüello SF, Lopez-Lorenzo B, Cornelissen B, et al. Development of [^{18}F]ICMT-11 for imaging caspase-3/7 activity during therapy-induced apoptosis. Cancers (Basel). 2020;12:E2191.

Nguyen QD, Challapalli A, Smith G, et al. Imaging apoptosis with positron emission tomography: 'bench to bedside' development of the caspase-3/7 specific radiotracer [^{18}F]ICMT-11. Eur J Cancer. 2012;48:432–40.

^{18}F-DCFPyL

Contents

Chemical name and alternative names	Chemical structure
(S)-2-[3-((S)-1-Carboxy-5-[3-(6-fluoropyridine)carbonyl)-amino)-pentyl) ureido]-pentanedioic acid; piflufolastat; PYLARIFY. PyL (Progenics/Lantheus)	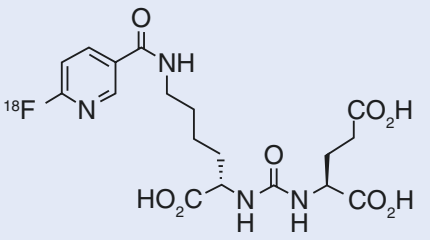

Route of Synthesis

The original synthesis involved preparation of an ^{18}F-fluoro-nicotinic acid active ester which was then coupled with protected urea derivative and purified. Recently, an alternative synthesis has been published which involves nucleophilic attack of ^{18}F-fluoride on a trimethylammonium precursor followed by acid hydrolysis of protecting groups and HPLC purification and dilution in acetate buffer (Bouvet et al. 2016).

Normal Biodistribution and Excretion

Rapid clearance from most tissues with highest levels in kidneys and liver. Salivary and lacrimal glands seen. Predominantly renal excretion with some activity in small intestine.

J. R. Ballinger, *PET Radiopharmaceuticals*, Clinicians' Guides to Radionuclide Hybrid Imaging, https://doi.org/10.1007/978-3-031-10271-4_15

Activity Administered

370 MBq.

Radiation Dosimetry

Effective dose equivalent (mSv/MBq): 0.017 (6 mSv/370 MBq).

Organ doses (mGy/MBq): kidneys, 0.095; urinary bladder wall, 0.086; submandibular glands, 0.039; liver, 0.038.

Patient Preparation

Patient preparation is not standardised yet.

Clinical Utility

Binds to prostate-specific membrane antigen. Evaluation of patients with suspected recurrent prostate cancer (Chen et al. 2011; Dietlein et al. 2015; Szabo et al. 2015; Wondergem et al. 2019).

Further Reading

Bouvet V, Wuest M, Jans HS, et al. Automated synthesis of [^{18}F]DCFPyL via direct radiofluorination and validation in preclinical prostate cancer models. EJNMMI Res. 2016;6:40.

Chen Y, Pullambhatla M, Foss CA, et al. 2-(3-{1-Carboxy-5-[(6-[^{18}F]fluoro-pyridine-3-carbonyl)-amino]-pentyl}-ureido)-pentanedioic acid, [^{18}F]DCFPyL, a PSMA-based PET imaging agent for prostate cancer. Clin Cancer Res. 2011;17:7645–53.

Dietlein M, Kobe C, Kuhnert G, Stockter S, et al. Comparison of [^{18}F]DCFPyL and [^{68}Ga]Ga-PSMA-HBED-CC for PSMA-PET imaging in patients with relapsed prostate cancer. Mol Imaging Biol. 2015;17:575–84.

Szabo Z, Mena E, Rowe SP, Plyku D, et al. Initial evaluation of [^{18}F]DCFPyL for prostate-specific membrane antigen (PSMA)-targeted PET imaging of prostate cancer. Mol Imaging Biol. 2015;17:565–74.

Wondergem M, Jansen BHE, van der Zant FM, et al. Early lesion detection with ^{18}F-DCFPyL PET/CT in 248 patients with biochemically recurrent prostate cancer. Eur J Nucl Med Mol Imaging. 2019;46:1911–8.

^{18}F-PSMA-1007

Contents

Chemical name and alternative names	Chemical structure
PSMA-1007 (ABX)	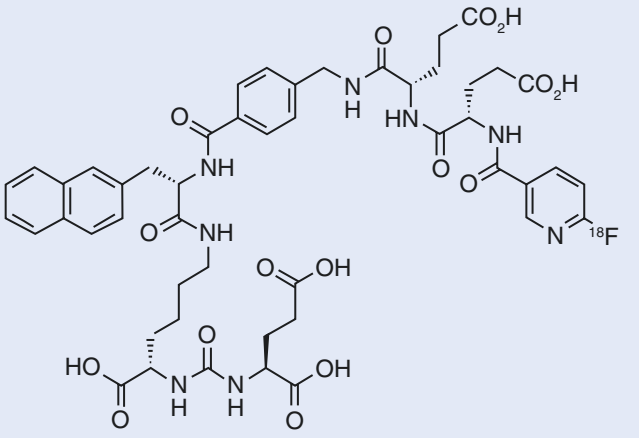

Route of Synthesis

Nucleophilic attack of ^{18}F-fluoride on an activated precursor followed by cartridge purification and reformulation (Cardinale et al. 2017).

Normal Biodistribution and Excretion

Following intravenous injection, PSMA-1007 is distributed throughout the body although after 60 min 22% of the administered activity still remains in the blood pool. Although the kidneys are prominent on whole body images, only 3.5% of the injected activity is recovered in the urine over 6 h (Giesel et al. 2017; Rahbar et al. 2018)).

J. R. Ballinger, *PET Radiopharmaceuticals*, Clinicians' Guides to Radionuclide Hybrid Imaging, https://doi.org/10.1007/978-3-031-10271-4_16

Activity Administered

250 MBq.

Radiation Dosimetry

Effective dose equivalent (mSv/MBq): 0.022 (5.5 mSv/250 MBq).

Organ doses (mGy/MBq): kidneys, 0.17; spleen, 0.074; liver, 0.060 (Giesel et al. 2017).

Patient Preparation

Patient preparation is not standardised yet.

Clinical Utility

Binds to prostate-specific membrane antigen. Evaluation of patients with suspected recurrent prostate cancer (Giesel et al. 2019; Foley et al. 2020).

Further Reading

Cardinale J, Martin R, Remde Y, et al. Procedures for the GMP-compliant production and quality control of [^{18}F]PSMA-1007: a next generation radiofluorinated tracer for the detection of prostate cancer. Pharmaceuticals (Basel). 2017;10:77.

Foley RW, Redman SL, Graham RN, et al. Fluorine-18 labelled prostate-specific membrane antigen (PSMA)-1007 positron-emission tomography-computed tomography: normal patterns, pearls, and pitfalls. Clin Radiol. 2020;75:903–13.

Giesel FL, Hadaschik B, Cardinale J, et al. F-18 labelled PSMA-1007: biodistribution, radiation dosimetry and histopathological validation of tumor lesions in prostate cancer patients. Eur J Nucl Med Mol Imaging. 2017;44:678–88.

Giesel FL, Knorr K, Spohn F, et al. Detection efficacy of ^{18}F-PSMA-1007 PET/CT in 251 patients with biochemical recurrence of prostate cancer after radical prostatectomy. J Nucl Med. 2019;60:362–8.

Rahbar K, Afshar-Oromieh A, Bögemann M, et al. ^{18}F-PSMA-1007 PET/CT at 60 and 120 minutes in patients with prostate cancer: biodistribution, tumour detection and activity kinetics. Eur J Nucl Med Mol Imaging. 2018;45:1329–1334.

^{18}F-Tetrafluoroborate

Contents

Chemical name and alternative names	Chemical structure
Sodium fluoroborate TFB	$NaBF_4$

Route of Synthesis

Exchange reaction between ^{18}F-fluoride and cold sodium tetrafluoroborate at elevated temperature followed by cartridge purification and sterile filtration. It is important to achieve moderately high specific activity to avoid saturation of the symporter (see below) (Jauregui-Osoro et al. 2010).

Normal Biodistribution and Excretion (Fig. 1)

Tetrafluoroborate is a substrate for the human sodium iodide symporter (hNIS). The thyroid gland is visible from the earliest time points, reaching a peak at 30 min. Accumulation is high in other organs which express hNIS, primarily the salivary glands and stomach. Excretion is primarily renal (O'Doherty et al. 2017).

Activity Administered

200–300 MBq.

Radiation Dosimetry

Effective dose equivalent (mSv/MBq): 0.033 (9.9 mSv/300 MBq).

Organ doses (mGy/MBq): thyroid, 0.14; urinary bladder wall, 0.10; stomach wall, 0.069; submandibular gland, 0.061 (Jiang et al. 2017).

J. R. Ballinger, *PET Radiopharmaceuticals*, Clinicians' Guides to Radionuclide Hybrid Imaging, https://doi.org/10.1007/978-3-031-10271-4_17

Patient Preparation

Patient preparation is not finalised yet.

Clinical Utility

As a substrate for hNIS, tetrafluoroborate might be useful to study thyroid disease including cancer. It offers the advantage over ^{124}I-iodide of much lower radiation dose. This favourable dosimetry may make it useful for reporter gene imaging. Although tetrafluoroborate is a substrate for hNIS, it is not organified and thus its retention may not be as durable as that of radioiodide (Samnick et al. 2018; Jiang et al. 2018).

Example Image

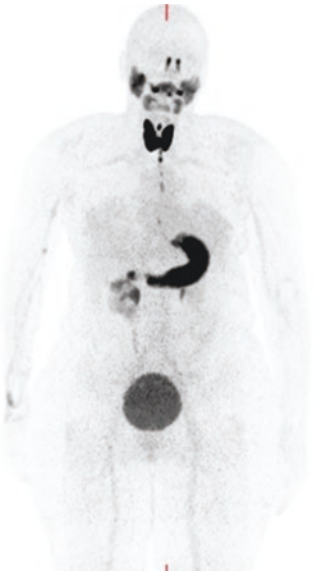

Fig. 1 Normal biodistribution of ^{18}F-tetrafluoroborate. Maximum intensity projection, anterior. *Image courtesy of Prof V Lewington, King's College London*

Further Reading

Jauregui-Osoro M, Sunassee K, Weeks AJ, et al. Synthesis and biological evaluation of [^{18}F]tetrafluoroborate: a PET imaging agent for thyroid disease and reporter gene imaging of the sodium/iodide symporter. Eur J Nucl Med Mol Imaging. 2010;37:2108–16.

Jiang H, DeGrado TR. [^{18}F]Tetrafluoroborate ([^{18}F]TFB) and its analogs for PET imaging of the sodium/iodide symporter. Theranostics. 2018;8:3918–3931.

Jiang H, Schmit NR, Koenen AR, et al. Safety, pharmacokinetics, metabolism and radiation dosimetry of ^{18}F-tetrafluoroborate (^{18}F-TFB) in healthy human subjects. EJNMMI Res. 2017;7:90.

O'Doherty J, Jauregui-Osoro M, Brothwood T, et al. ^{18}F-Tetrafluoroborate, a PET probe for imaging sodium/iodide symporter expression: whole-body biodistribution, safety, and radiation dosimetry in thyroid cancer patients. J Nucl Med. 2017;58:1666–1671.

Samnick S, Al-Momani E, Schmid JS, et al. Initial clinical investigation of [^{18}F]tetrafluoroborate PET/CT in comparison to [^{124}I]iodine PET/CT for imaging thyroid cancer. Clin Nucl Med. 2018;43:162–7.

Part II

Oncology—^{11}C-Labelled Agents

^{11}C-Acetate

Contents

Chemical name and alternative names	Chemical structure
Sodium acetate	CH_3–$^{11}CO_2^-$

Route of Synthesis

Reaction of ^{11}C-CO_2 with methyl magnesium bromide or chloride, followed by hydrolysis and purification.

Normal Biodistribution and Excretion

Taken up in proportion to fatty acid synthesis in most tissues and myocardial perfusion in the heart. Clears from most tissues except pancreas within 20–30 min, allowing visualisation of tumours. No urinary excretion.

Activity Administered

740–1480 MBq.

Radiation Dosimetry

Effective dose equivalent (mSv/MBq): 0.0062.

Organ doses (mGy/MBq): pancreas, 0.017; intestines, 0.011; kidneys, 0.0092; spleen, 0.0092.

J. R. Ballinger, *PET Radiopharmaceuticals*, Clinicians' Guides to Radionuclide Hybrid Imaging, https://doi.org/10.1007/978-3-031-10271-4_18

Patient Preparation

No special preparation required.

Clinical Utility

Enzymatic conversion of ^{11}C-acetate to ^{11}C-acetyl-CoA then converted into fatty acids. These are then either incorporated into cellular membranes in proportion to cellular proliferation rate (e.g. in tumours) or oxidised via tricarboxylic acid cycle in normal myocardium. Taken up in prostate cancer and metastases, though may also be seen in benign or hyperplastic prostate tissue. Also useful to study fatty acid metabolism in the heart (Armbrecht et al. 1989; Grassi et al. 2012; Nesterov et al. 2015).

Further Reading

Armbrecht JJ, Buxton DB, Brunken RC, et al. Regional myocardial oxygen consumption determined noninvasively in humans with [1-^{11}C]acetate and dynamic positron tomography. Circulation. 1989;80:863–72.

Grassi I, Nanni C, Allegri V, et al. The clinical use of PET with ^{11}C-acetate. Am J Nucl Med Mol Imaging. 2012;2:33–47.

Nesterov SV, Turta O, Han C, et al. C-11 acetate has excellent reproducibility for quantification of myocardial oxidative metabolism. Eur Heart J Cardiovasc Imaging. 2015;16:500–6.

^{11}C-Choline

Contents

Chemical name and alternative names	Chemical structure
2-Hydroxy-*N*,*N*-dimethyl-*N*-(methyl-[^{11}C])-ethanaminium chloride, ^{11}C-(2-hydroxyethyl)-trimethylammonium chloride	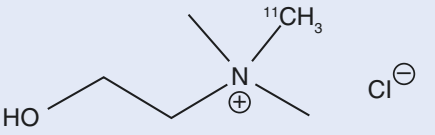

Route of Synthesis

Cyclotron-produced $^{11}C–CO_2$ is reduced to $^{11}C–CH_4$, then iodinated to $^{11}C–CH_3I$. The latter reacts with the precursor, *N*,*N*-dimethylaminoethanol, to form ^{11}C-choline. In one of the synthetic routes, the precursor is loaded onto a C-18 solid phase extraction cartridge. After the reaction, the product is trapped on a cation exchange cartridge, washed with water, and eluate with normal saline.

Normal Biodistribution and Excretion

Distributed rapidly to liver, spleen, pancreas, renal cortex, salivary glands, and muscle. Less than 2% excretion in urine (Tolvanen et al. 2010).

Activity Administered

400 MBq.

J. R. Ballinger, *PET Radiopharmaceuticals*, Clinicians' Guides to Radionuclide Hybrid Imaging, https://doi.org/10.1007/978-3-031-10271-4_19

Radiation Dosimetry

Effective dose equivalent (mSv/MBq): 0.0044 (2 mSv/400 MBq).

Organ doses (mGy/MBq): kidneys, 0.021; liver, 0.020; pancreas, 0.029 (Tolvanen et al. 2010).

Patient Preparation

No special preparation required.

Clinical Utility

Phospholipid synthesis in tumours. Particularly useful in prostate cancer due to low excretion in urine (Murphy et al. 2011; Treglia et al. 2012; Nanni et al. 2016).

Further Reading

Murphy RC, Kawashima A, Peller PJ. The utility of ^{11}C-choline PET/CT for imaging prostate cancer: a pictorial guide. AJR Am J Roentgenol. 2011;196:1390–8.

Nanni C, Zanoni L, Pultrone C, et al. ^{18}F-FACBC (anti 1-amino-3-^{18}F-fluorocyclobutane-1-carboxylic acid) versus ^{11}C-choline PET/CT in prostate cancer relapse: results of a prospective trial. Eur J Nucl Med Mol Imaging. 2016;43:1601–1610.

Tolvanen T, Yli-Kerttula T, Ujula T, et al. Biodistribution and radiation dosimetry of [^{11}C]choline: a comparison between rat and human data. Eur J Nucl Med Mol Imaging. 2010;37:874–83.

Treglia G, Giovannini E, Di Franco D, et al. The role of positron emission tomography using carbon-11 and fluorine-18 choline in tumors other than prostate cancer: a systematic review. Ann Nucl Med. 2012;26:451–61.

^{11}C-Methionine

Contents

Chemical name and alternative names	Chemical structure
L-methionine, ^{11}C-Met	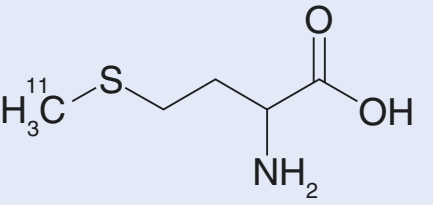

Route of Synthesis

Cyclotron-produced $^{11}C–CO_2$ is reduced to $^{11}C–CH_4$, then iodinated to $^{11}C–CH_3I$. The latter reacts with the precursor, L-homocysteine, to form ^{11}C-methionine. In one of the synthetic routes, the precursor is loaded onto an anion exchange solid phase extraction cartridge. After the reaction, the cartridge is washed with water followed by ethanol, and the product is eluted with normal saline.

Normal Biodistribution and Excretion

Highest activity in liver, pancreas, kidney, and bladder.

Activity Administered

370 MBq.

J. R. Ballinger, *PET Radiopharmaceuticals*, Clinicians' Guides to Radionuclide Hybrid Imaging, https://doi.org/10.1007/978-3-031-10271-4_20

Radiation Dosimetry

Effective dose equivalent (mSv/MBq): 0.0052 (1.9 mSv/370 MBq).

Organ doses (mGy/MBq): bladder wall, 0.027; pancreas, 0.019; liver, 0.018; kidney, 0.011 (Deloar et al. 1998).

Patient Preparation

No special preparation required.

Clinical Utility

Protein synthesis in tumours, particularly glioma and non-small cell lung cancer (Hsieh et al. 2008; Glaudemans et al. 2013; Wang et al. 2018).

Further Reading

Deloar HM, Fujiwara T, Nakamura T, et al. Estimation of internal absorbed dose of L-[methyl-^{11}C]methionine using whole-body positron emission tomography. Eur J Nucl Med. 1998;25:629–33.

Glaudemans AW, Enting RH, Heesters MA, et al. Value of ^{11}C-methionine PET in imaging brain tumours and metastases. Eur J Nucl Med Mol Imaging. 2013;40:615–35.

Hsieh HJ, Lin SH, Lin KH, et al. The feasibility of ^{11}C-methionine-PET in diagnosis of solitary lung nodules/masses when compared with ^{18}F-FDG-PET. Ann Nucl Med. 2008;22:533–8.

Wang Y, Rapalino O, Heidari P, et al. C11 methionine PET (MET-PET) imaging of glioblastoma for detecting postoperative residual disease and response to chemoradiation therapy. Int J Radiat Oncol Biol Phys. 2018;102:1024–8.

Part III

Oncology—^{68}Ga-Labelled Agents

^{68}Ga-DOTATOC

Contents

Chemical name and alternative names	Chemical structure
Edotreotide; DOTA-Tyr^3-octreotide; SomaKit-TOC (AAA)	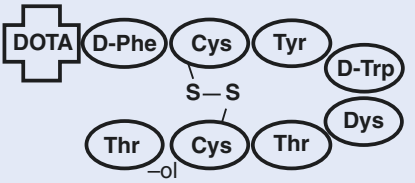

Route of Synthesis

Chelation of generator-produced ^{68}Ga-chloride by DOTATOC at elevated temperature. May be preceded or followed by purification step.

Normal Biodistribution and Excretion (Fig. 1)

Activity initially high in liver, spleen, and kidneys. Gradual clearance with 16% urinary excretion over 4 h (Sandström et al. 2013).

Activity Administered

100–150 MBq.

Radiation Dosimetry

Effective dose equivalent (mSv/MBq): 0.021 (2 mSv/100 MBq).

J. R. Ballinger, *PET Radiopharmaceuticals*, Clinicians' Guides to Radionuclide Hybrid Imaging, https://doi.org/10.1007/978-3-031-10271-4_21

Organ doses (mGy/MBq): urinary bladder wall, 0.119; spleen, 0.108; kidney, 0.082; adrenal gland, 0.077 (Sandström et al. 2013).

Patient Preparation

Withdraw therapeutic somatostatin analogues.

Clinical Utility

Assessment of somatostatin receptor status of neuroendocrine tumours, particularly in selection of patients for radiopeptide therapy (Virgolini et al. 2010; Graham et al. 2017).

Example Image

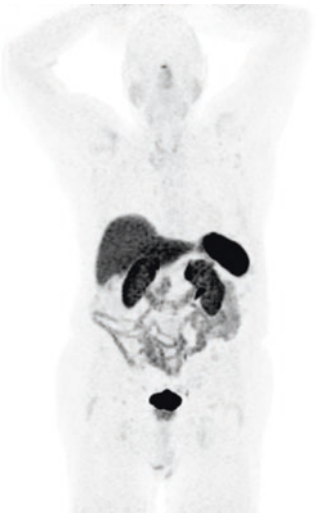

Fig. 1 Normal biodistribution of ^{68}Ga-DOTATOC. Maximum intensity projection, anterior

Further Reading

Graham MM, Gu X, Ginader T, et al. ^{68}Ga-DOTATOC imaging of neuroendocrine tumors: a systematic review and metaanalysis. J Nucl Med. 2017;58:1452–1458.

Sandström M, Velikyan I, Garske-Román U, et al. Comparative biodistribution and radiation dosimetry of ^{68}Ga-DOTATOC and ^{68}Ga-DOTATATE in patients with neuroendocrine tumors. J Nucl Med. 2013;54:1755–9.

Virgolini I, Ambrosini V, Bomanji JB, et al. Procedure guidelines for PET/CT tumour imaging with ^{68}Ga-DOTA-conjugated peptides: ^{68}Ga-DOTA-TOC, ^{68}Ga-DOTA-NOC, ^{68}Ga-DOTA-TATE. Eur J Nucl Med Mol Imaging. 2010;37:2004–10.

^{68}Ga-DOTATATE

Contents

Chemical name and alternative names	Chemical structure
Oxodotreotide; DOTA-Tyr^3-octreotate; Netspot; SomaKit-TATE (AAA)	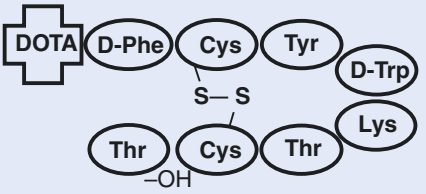

Route of Synthesis

Chelation of generator-produced ^{68}Ga-chloride by DOTATATE at elevated temperature. May be preceded or followed by purification step.

Normal Biodistribution and Excretion (Fig. 1)

Activity initially high in liver, spleen, and kidneys. Gradual clearance with 12% urinary excretion over 4 h (Sandström et al. 2013).

Activity Administered

100–150 MBq.

Radiation Dosimetry

Effective dose equivalent (mSv/MBq): 0.021 (2 mSv/100 MBq).

Organ doses (mGy/MBq): spleen, 0.109; urinary bladder wall, 0.098; kidney, 0.093; adrenal gland, 0.086 (Walker et al. 2013; Sandström et al. 2013).

J. R. Ballinger, *PET Radiopharmaceuticals*, Clinicians' Guides to Radionuclide Hybrid Imaging, https://doi.org/10.1007/978-3-031-10271-4_22

Patient Preparation

Withdraw therapeutic somatostatin analogues.

Clinical Utility

Assessment of somatostatin receptor status of neuroendocrine tumours, particularly in selection of patients for radiopeptide therapy (Virgolini et al., 2010; Sanli et al., 2018).

Example Image

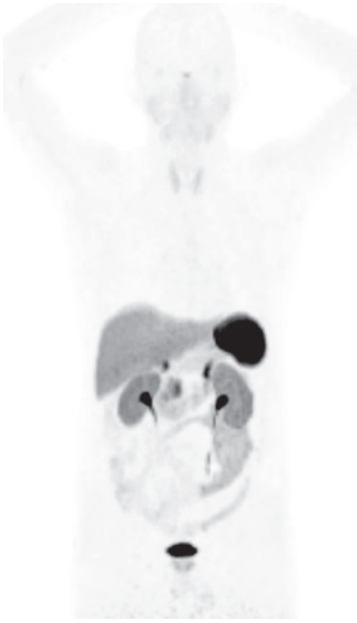

Fig. 1 Normal biodistribution of ^{68}Ga-DOTATATE. Maximum intensity projection, anterior

Further Reading

Sandström M, Velikyan I, Garske-Román U, et al. Comparative biodistribution and radiation dosimetry of ^{68}Ga-DOTATOC and ^{68}Ga-DOTATATE in patients with neuroendocrine tumors. J Nucl Med. 2013;54:1755–9.

Sanli Y, Garg I, Kandathil A, et al. Neuroendocrine tumor diagnosis and management: ^{68}Ga-DOTATATE PET/CT. AJR Am J Roentgenol. 2018;211:267–77.

Virgolini I, Ambrosini V, Bomanji JB, et al. Procedure guidelines for PET/CT tumour imaging with ^{68}Ga-DOTA-conjugated peptides: ^{68}Ga-DOTA-TOC, ^{68}Ga-DOTA-NOC, ^{68}Ga-DOTA-TATE. Eur J Nucl Med Mol Imaging. 2010;37:2004–10.

Walker RC, Smith GT, Liu E, et al. Measured human dosimetry of ^{68}Ga-DOTATATE. J Nucl Med. 2013;54:855–60.

^{68}Ga-HA-DOTATATE

Contents

Chemical name and alternative names	Chemical structure
High affinity DOTATATE; DOTA-[3-iodoTyr^3]-octreotate (Scintomics)	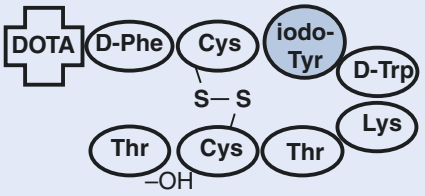

Route of Synthesis

Chelation of generator-produced ^{68}Ga-chloride by HA-DOTATATE at elevated temperature. May be preceded or followed by purification step.

Normal Biodistribution and Excretion (Fig. 1)

Activity initially high in liver, spleen, and kidneys.

Activity Administered

100–150 MBq.

Radiation Dosimetry

Effective dose equivalent (mSv/MBq): 0.024 (2.4 mSv/100 MBq).

J. R. Ballinger, *PET Radiopharmaceuticals*, Clinicians' Guides to Radionuclide Hybrid Imaging, https://doi.org/10.1007/978-3-031-10271-4_23

Organ doses (mGy/MBq): spleen, 0.26; kidney, 0.14; liver, 0.12 (Hartmann et al. 2014).

Patient Preparation

Withdraw therapeutic somatostatin analogues.

Clinical Utility

Assessment of somatostatin receptor status of neuroendocrine tumours, particularly in selection of patients for radiopeptide therapy (Brogsitter et al. 2014; Bodei et al. 2014).

Example Image

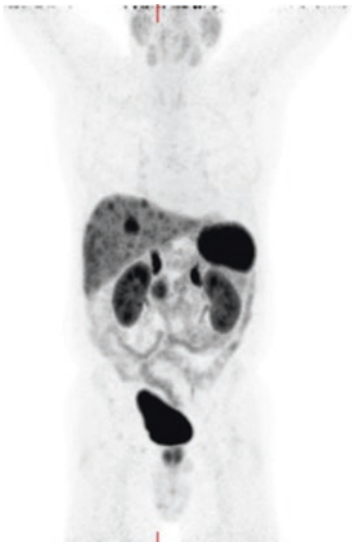

Fig. 1 Normal biodistribution of ^{68}Ga-HA-DOTATATE. Maximum intensity projection, anterior. *Image courtesy of Prof G Cook, King's College London*

Further Reading

Bodei L, Kidd M, Prasad V, et al. The future of nuclear medicine imaging of neuroendocrine tumors: on a clear day one might see forever. Eur J Nucl Med Mol Imaging. 2014;41:2189–93.

Brogsitter C, Zöphel K, Hartmann H, et al. Twins in spirit part II: DOTATATE and high-affinity DOTATATE—the clinical experience. Eur J Nucl Med Mol Imaging. 2014;41:1158–65.

Hartmann H, Freudenberg R, Oehme L, et al. Dosimetric measurements of ^{68}Ga-high affinity DOTATATE. Twins in spirit—part III. Nuklearmedizin. 2014;53:211–6.

^{68}Ga-DOTANOC

Contents

Chemical name and alternative names	Chemical structure
DOTA-Nal^3-octreotide	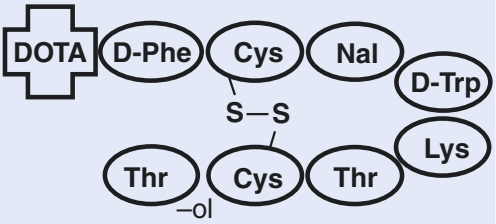

Route of Synthesis

Chelation of generator-produced ^{68}Ga-chloride by DOTANOC at elevated temperature. May be preceded or followed by purification step.

Normal Biodistribution and Excretion (Fig. 1)

Activity initially high in liver, spleen, and kidneys. Gradual clearance with 25% urinary excretion over 4 h (Pettinato et al. 2008).

Activity Administered

100–150 MBq.

Radiation Dosimetry

Effective dose equivalent (mSv/MBq): 0.025 (2.5 mSv/100 MBq).

Organ doses (mGy/MBq): kidney, 0.090; urinary bladder wall, 0.084; spleen, 0.073; liver, 0.034 (Pettinato et al. 2008).

J. R. Ballinger, *PET Radiopharmaceuticals*, Clinicians' Guides to Radionuclide Hybrid Imaging, https://doi.org/10.1007/978-3-031-10271-4_24

Patient Preparation

Withdraw therapeutic somatostatin analogues.

Clinical Utility

Assessment of somatostatin receptor status of neuroendocrine tumours, particularly in selection of patients for radiopeptide therapy (Virgolini et al. 2010; Kagna et al. 2014; Singh et al. 2020).

Example Image

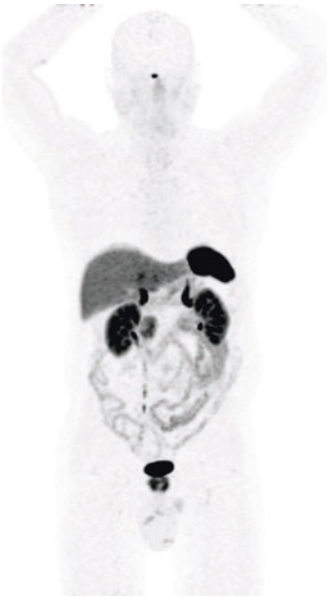

Fig. 1 Normal biodistribution of ^{68}Ga-DOTANOC. Maximum intensity projection, anterior

Further Reading

Kagna O, Pirmisashvili N, Tshori S, et al. Neuroendocrine tumor imaging with ^{68}Ga-DOTA-NOC: physiologic and benign variants. AJR Am J Roentgenol. 2014;203:1317–23.

Pettinato C, Sarnelli A, Di Donna M, et al. ^{68}Ga-DOTANOC: biodistribution and dosimetry in patients affected by neuroendocrine tumors. Eur J Nucl Med Mol Imaging. 2008;35:72–79.

Singh D, Shukla J, Walia R, et al. Role of [^{68}Ga]DOTANOC PET/computed tomography and [^{131}I]MIBG scintigraphy in the management of patients with pheochromocytoma and paraganglioma: a prospective study. Nucl Med Commun. 2020;41(10):1047–59.

Virgolini I, Ambrosini V, Bomanji JB, et al. Procedure guidelines for PET/CT tumour imaging with ^{68}Ga-DOTA-conjugated peptides: ^{68}Ga-DOTA-TOC, ^{68}Ga-DOTA-NOC, ^{68}Ga-DOTA-TATE. Eur J Nucl Med Mol Imaging. 2010;37:2004–10.

^{68}Ga-DKFZ-PSMA-11

Contents

Chemical name and alternative names	Chemical structure
PSMA-HBED-CC; Glu-NH-CO-NHLys-(Ahx)-[^{68}Ga(HBED-CC)]; Gozetotide; TLX591-CDx; Illuccix (Telix); Locametz (Novartis)	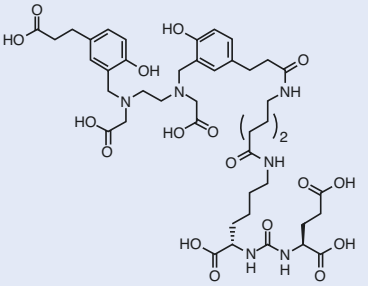

Route of Synthesis

Chelation of generator- or cyclotron-produced ^{68}Ga-chloride by DKFZ-PSMA-11 at ambient temperature. May be preceded or followed by purification step (Eder et al. 2014).

Normal Biodistribution and Excretion (Fig. 1)

Highest activities seen in the kidneys, salivary glands, liver, spleen, and proximal small intestine (Afshar-Oromieh et al. 2013).

Activity Administered

110–260 MBq (2 MBq/kg).

Radiation Dosimetry

Effective dose equivalent (mSv/MBq): 0.017 (3 mSv/150 MBq).

Organ doses (mGy/MBq): kidney, 0.37; urinary bladder, 0.10; spleen, 0.07; liver, 0.04.

J. R. Ballinger, *PET Radiopharmaceuticals*, Clinicians' Guides to Radionuclide Hybrid Imaging, https://doi.org/10.1007/978-3-031-10271-4_25

Patient Preparation

Patient should be well hydrated.

Clinical Utility

Binds to prostate-specific membrane antigen. Evaluation of patients with suspected recurrent prostate cancer, particularly those underconsideration for therapy with PSMA-directed ^{177}Lu-labelled radiotherapeutics (Afshar-Oromieh et al. 2015, 2016).

Example Image

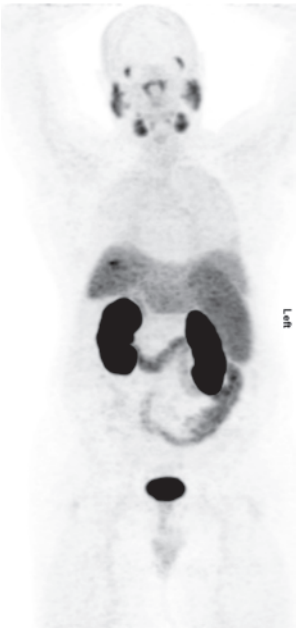

Fig. 1 Normal biodistribution of ^{68}Ga-PSMA-11. Maximum intensity projection, anterior

Further Reading

Afshar-Oromieh A, Malcher A, Eder M, et al. PET imaging with a [^{68}Ga]gallium-labelled PSMA ligand for the diagnosis of prostate cancer: biodistribution in humans and first evaluation of tumour lesions. Eur J Nucl Med Mol Imaging. 2013;40:486–95.

Afshar-Oromieh A, Avtzi E, Giesel FL, et al. The diagnostic value of PET/CT imaging with the ^{68}Ga-labelled PSMA ligand HBED-CC in the diagnosis of recurrent prostate cancer. Eur J Nucl Med Mol Imaging. 2015;42:197–209.

Afshar-Oromieh A, Hetzheim H, Kübler W, et al. Radiation dosimetry of ^{68}Ga-PSMA-11 (HBED-CC) and preliminary evaluation of optimal imaging timing. Eur J Nucl Med Mol Imaging. 2016;43:1611–20.

Eder M, Neels O, Müller M, et al. Novel preclinical and radiopharmaceutical aspects of [^{68}Ga]Ga-PSMA-HBED-CC: a new PET tracer for imaging of prostate cancer. Pharmaceuticals. 2014;7:779–96.

^{68}Ga-THP-PSMA

Contents

Chemical name and alternative names	Chemical structure
Tris(hydroxypyridinone)-PSMA; GalliProst (Theragnostics/GE Healthcare)	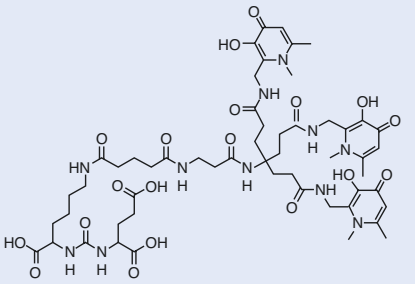

Route of Synthesis

Addition of generator-produced ^{68}Ga-chloride in dilute HCl to a sterile kit containing THP-PSMA and a buffer. Quantitative labelling takes place within 5 min at room temperature and no purification is required (Young et al. 2017).

Normal Biodistribution and Excretion (Fig. 1)

Physiologic uptake is seen in the lacrimal glands, salivary glands, liver, spleen, and duodenum although the intensity of uptake in these organs is low. High kidney, ureter, and bladder activities are seen because of the extensive renal excretion of the tracer.

Activity Administered

150 MBq.

J. R. Ballinger, *PET Radiopharmaceuticals*, Clinicians' Guides to Radionuclide Hybrid Imaging, https://doi.org/10.1007/978-3-031-10271-4_26

Radiation Dosimetry

Effective dose equivalent (mSv/MBq): 0.021 (3.2 mSv/150 MBq).
Organ doses (mGy/MBq): urinary bladder, 0.23; kidneys, 0.08.

Patient Preparation

No specific preparation except bladder voiding immediately before imaging.

Clinical Utility

Useful in making clinical management decisions in patients with high-risk prostate cancer before radical treatment and in patients with biochemical recurrence (Hofman et al. 2018; Kulkarni et al. 2020).

Example Image

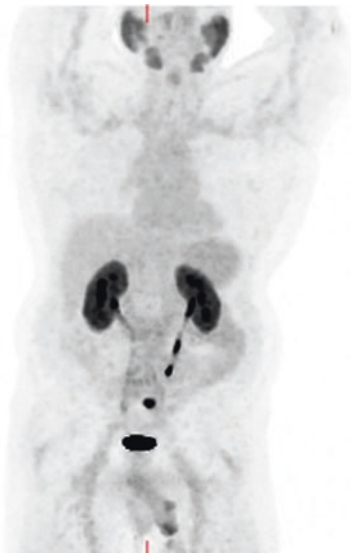

Fig. 1 Normal biodistribution of ^{68}Ga-THP-PSMA. Maximum intensity projection, anterior. *Image courtesy of Prof G Cook, King's College London*

Further Reading

Hofman MS, Eu P, Jackson P, et al. Cold kit for prostate-specific membrane antigen (PSMA) PET imaging: phase 1 study of ^{68}Ga-tris(hydroxypyridinone)-PSMA PET/CT in patients with prostate cancer. J Nucl Med. 2018;59:625–31.

Kulkarni M, Hughes S, Mallia A, et al. The management impact of ^{68}gallium-tris(hydroxypyridinone) prostate-specific membrane antigen (^{68}Ga-THP-PSMA) PET-CT imaging for high-risk and biochemically recurrent prostate cancer. Eur J Nucl Med Mol Imaging. 2020;47:674–86.

Young JD, Abbate V, Imberti C, et al. ^{68}Ga-THP-PSMA: a PET imaging agent for prostate cancer offering rapid, room-temperature, 1-step kit-based radiolabeling. J Nucl Med. 2017;58:1270–1277.

^{68}Ga-NOTA-RGD

Contents

Chemical name and alternative names	Chemical structure
^{68}Ga-1,4,7-Triazacyclononane-1,4–7-triacetic acid-isothiocyanatobenzyl-c (Arg-Gly-asp-d-Tyr-Lys); ^{68}Ga-NOTA-SCN-Bz-c(RGDyK)	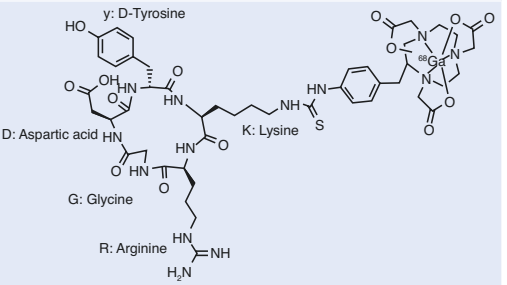

Route of Synthesis

Chelation of generator-produced ^{68}Ga-chloride by NOTA-RGD at elevated temperature, followed by purification through an alumina solid phase extraction cartridge and sterilisation by membrane filtration (Jeong et al. 2008).

Normal Biodistribution and Excretion

High levels of activity in kidneys and bladder, also in the liver (Kim et al. 2012; Ebenhan et al. 2017).

Activity Administered

200 MBq.

J. R. Ballinger, *PET Radiopharmaceuticals*, Clinicians' Guides to Radionuclide Hybrid Imaging, https://doi.org/10.1007/978-3-031-10271-4_27

Radiation Dosimetry

Effective dose equivalent (mSv/MBq): 0.022 (4.4 mSv/200 MBq).
Organ doses (mGy/MBq): urinary bladder, 0.24; kidneys, 0.072 (Kim et al. 2012).

Patient Preparation

No specific preparation required.

Clinical Utility

Targets $\alpha_v\beta_3$ integrin for imaging angiogenesis. Has been shown to be taken up in breast cancer (Yoon et al. 2014; Kim et al. 2016).

Further Reading

Ebenhan T, Schoeman I, Rossouw DD, et al. Evaluation of a flexible NOTA-RGD kit solution using gallium-68 from different ^{68}Ge/^{68}Ga-generators: pharmacokinetics and biodistribution in nonhuman primates and demonstration of solitary pulmonary nodule imaging in humans. Mol Imaging Biol. 2017;19:469–82.

Jeong JM, Hong MK, Chang YS, et al. Preparation of a promising angiogenesis PET imaging agent: ^{68}Ga-labeled c(RGDyK)-isothiocyanatobenzyl-1,4,7-triazacyclononane-1,4,7-triacetic acid and feasibility studies in mice. J Nucl Med. 2008;49:830–6.

Kim JH, Lee JS, Kang KW, et al. Whole-body distribution and radiation dosimetry of ^{68}Ga-NOTA-RGD, a positron emission tomography agent for angiogenesis imaging. Cancer Biother Radiopharm. 2012;27:65–71.

Kim YI, Yoon HJ, Paeng JC, et al. Prognostic value of ^{68}Ga-NOTA-RGD PET/CT for predicting disease-free survival for patients with breast cancer undergoing neoadjuvant chemotherapy and surgery: a comparison study with dynamic contrast enhanced MRI. Clin Nucl Med. 2016;41:614–20.

Yoon HJ, Kang KW, Chun IK, et al. Correlation of breast cancer subtypes, based on estrogen receptor, progesterone receptor, and HER2, with functional imaging parameters from ^{68}Ga-RGD PET/CT and ^{18}F-FDG PET/CT. Eur J Nucl Med Mol Imaging. 2014;41:1534–43.

^{68}Ga-NODAGA-RGD

Contents

Chemical name and alternative names	Chemical structure
NODAGA-cyclo(RGDyK); cyclo[-Arg-Gly-asp-D-Tyr-Lys(NODAGA)-]; cyclo[L-arginylglycyl-L-α-aspartyl-D-tyrosyl-N6-([[4,7-bis(carboxymethyl)-1,4,7-triazonan-1-yl]acetyl])-L-lysyl]; ^{68}Ga-1,4,7-Triazacyclononane,1-glutaric acid-4,7-acetic acid-cyclo(Arg-Gly-asp-d-Phe-Lys)	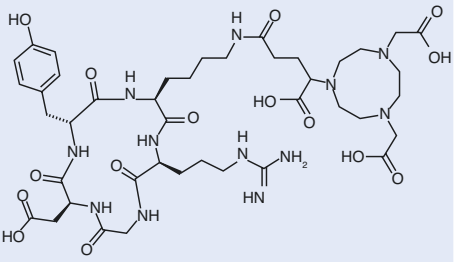

Route of Synthesis

Chelation of generator-produced ^{68}Ga-chloride by NODAGA-RGD at elevated temperature. May be preceded or followed by purification step (Pohle et al. 2012).

Normal Biodistribution and Excretion

Rapid distribution with predominantly renal excretion. High levels of activity in kidneys and bladder, also in the liver and spleen. No metabolites have been detected in blood or urine (Haubner et al. 2016).

Activity Administered

150–200 MBq.

J. R. Ballinger, *PET Radiopharmaceuticals*, Clinicians' Guides to Radionuclide Hybrid Imaging, https://doi.org/10.1007/978-3-031-10271-4_28

Radiation Dosimetry

Effective dose equivalent (mSv/MBq): 0.022 (4.3 mSv/200 MBq).

Organ doses (mGy/MBq): urinary bladder, 0.26; kidneys, 0.069; spleen, 0.048 (Haubner et al. 2016).

Patient Preparation

No specific preparation required.

Clinical Utility

Targets $\alpha_v\beta_3$ integrin for imaging angiogenesis. Phase I study failed to show accumulation in hepatocellular carcinoma (Knetsch et al. 2011; Durante et al. 2020).

Further Reading

Durante S, Dunet V, Gorostidi F, et al. Head and neck tumors angiogenesis imaging with ^{68}Ga-NODAGA-RGD in comparison to ^{18}F-FDG PET/CT: a pilot study. EJNMMI Res. 2020;10:47.

Haubner R, Finkenstedt A, Stegmayr A, et al. [^{68}Ga]NODAGA-RGD–Metabolic stability, biodistribution, and dosimetry data from patients with hepatocellular carcinoma and liver cirrhosis. Eur J Nucl Med Mol Imaging. 2016;43:2005–13.

Knetsch PA, Petrik M, Griessinger CM, et al. [^{68}Ga]NODAGA-RGD for imaging αvβ3 integrin expression. Eur J Nucl Med Mol Imaging. 2011;38:1303–12.

Pohle K, Notni J, Bussemer J, et al. ^{68}Ga-NODAGA-RGD is a suitable substitute for ^{18}F-Galacto-RGD and can be produced with high specific activity in a cGMP/GRP compliant automated process. Nucl Med Biol. 2012;39:777–84.

^{68}Ga-DOTA-Zoledronate

Contents

Chemical name and alternative names	Chemical structure
2,2′,2″-(10-(2-((2-(1-(2-hydroxy-2,2-diphosphono-ethyl)-1H-imidazol-4-yl) ethyl)-amino)-2-oxoethyl)-1,4,7,10-tetraazacyclo-dodecane-1,4,7-triyl) triacetic acid DOTA-ZOL; DOTA^{ZOL}	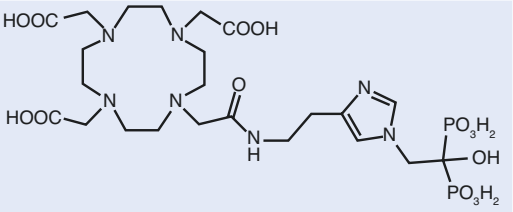

Route of Synthesis

Chelation of generator produced ^{68}Ga-chloride with DOTA-zoledronate in acetate buffer at elevated temperature, followed by cartridge purification (Meckel et al. 2017).

Normal Biodistribution and Excretion

High accumulation is seen in the skeleton as biological target and kidneys and bladder as organs of excretion. Faint accumulation is seen in liver, spleen, and salivary glands. Activity is seen in the renal parenchyma within 2.5 min of injection, but renal clearance is rapid and only minimal activity is evident at 45 min (Khawar et al. 2019).

Activity Administered

150 MBq.

J. R. Ballinger, *PET Radiopharmaceuticals*, Clinicians' Guides to Radionuclide Hybrid Imaging, https://doi.org/10.1007/978-3-031-10271-4_29

Radiation Dosimetry

Effective dose equivalent (mSv/MBq): 0.017 (2.6 mSv/150 MBq).

Organ doses (mGy/MBq): urinary bladder wall, 0.37; osteogenic cells, 0.040; kidneys, 0.031 (Khawar et al. 2019).

Patient Preparation

The patient should be well hydrated to reduce the radiation dose to the kidneys and bladder.

Clinical Utility

It is anticipated that utility will be similar to ^{18}F-fluoride (though with much reduced radiation dose) and the ^{99m}Tc diphosphonate bone scan agents. In particular, may be useful prior to palliative therapy with ^{177}Lu- or ^{225}Ac-DOTA-ZOL (Meisenheimer et al. 2020).

Further Reading

Khawar A, Eppard E, Roesch F, et al. Preliminary results of biodistribution and dosimetric analysis of [^{68}Ga]Ga-DOTA^{ZOL}: a new zoledronate-based bisphosphonate for PET/CT diagnosis of bone diseases. Ann Nucl Med. 2019;33:404–13.

Meckel M, Bergmann R, Miederer M, et al. Bone targeting compounds for radiotherapy and imaging: *me(III)-DOTA conjugates of bisphosphonic acid, pamidronic acid and zoledronic acid. EJNMMI Radiopharm Chem. 2017;1:14.

Meisenheimer M, Kürpig S, Essler M, et al. DOTA-ZOL: a promising tool in diagnosis and palliative therapy of bone metastasis–challenges and critical points in implementation into clinical routine. Molecules. 2020;25:2988.

^{68}Ga-DOTA-Bombesin

Contents

Chemical name and alternative names	Chemical structure
DOTA-4-amino-1-carboxymethyl-piperidine-d-Phe-Gln-Trp-ala-Val-Gly-his-Sta-Leu-NH2 BAY86–7548 RM2	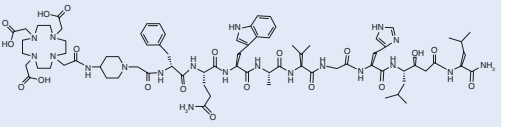

Route of Synthesis

Chelation of generator produced ^{68}Ga-chloride with DOTA-RM2 in acetate buffer at elevated temperature, followed by cartridge purification (Mansi et al. 2011).

Normal Biodistribution and Excretion

RM2 is a synthetic bombesin receptor antagonist which targets the gastrin-releasing peptide receptor (GRPR). The tracer shows rapid accumulation in the pancreas, as well as clearance via the kidneys into the bladder, with 38% of the activity reaching the bladder within 10 min (Haendeler et al. 2019).

Activity Administered

150 MBq.

J. R. Ballinger, *PET Radiopharmaceuticals*, Clinicians' Guides to Radionuclide Hybrid Imaging, https://doi.org/10.1007/978-3-031-10271-4_30

Radiation Dosimetry

Effective dose equivalent (mSv/MBq): 0.031 (4.7 mSv/150 MBq).

Organ doses (mGy/MBq): urinary bladder wall, 0.29; pancreas, 0.13; stomach wall, 0.094; kidneys, 0.047 (Haendeler et al. 2019).

Patient Preparation

No specific preparation required.

Clinical Utility

The gastrin-releasing peptide receptor is overexpressed in a range of cancers where it reflects proliferation. Initial evaluation of RM2 has been in prostate and breast cancer (Minamimoto et al. 2016, 2018).

Further Reading

Haendeler M, Khawar A, Kuerpig S, et al. Biodistribution and radiation dosimetry of [^{68}Ga]Ga-RM2. Nuklearmedizin. 2019;58:152.

Mansi R, Wang X, Forrer F, et al. Development of a potent DOTA-conjugated bombesin antagonist for targeting GRPr-positive tumours. Eur J Nucl Med Mol Imaging. 2011;38:97–107.

Minamimoto R, Hancock S, Schneider B, et al. Pilot comparison of ^{68}Ga-RM2 PET and ^{68}Ga-PSMA-11 PET in patients with biochemically recurrent prostate cancer. J Nucl Med. 2016;57:557–62.

Minamimoto R, Sonni I, Hancock S, et al. Prospective evaluation of ^{68}Ga-RM2 PET/MRI in patients with biochemical recurrence of prostate cancer and negative findings on conventional imaging. J Nucl Med. 2018;59:803–8.

^{68}Ga-NOTA-Bombesin

Contents

Chemical name and alternative names	Chemical structure
^{68}Ga-1,4,7-triazacyclononane-*N*,*N*′,*N*″-triacetic acid-D-Phe-Gln-Trp-ala-Val-Gly-his-Sta-Leu-NH2 RM26	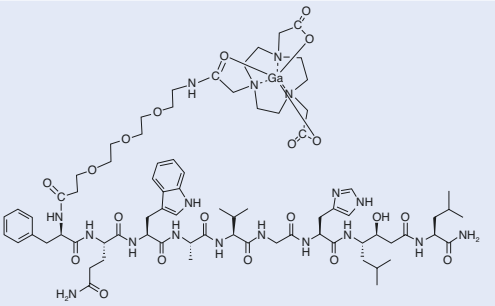

Route of Synthesis

Chelation of generator produced ^{68}Ga-chloride with NOTA-RM26 in acetate buffer at elevated temperature, followed by sterile filtration (Varasteh et al. 2013).

Normal Biodistribution and Excretion

RM26, a synthetic bombesin analogue and antagonist of the gastrin-releasing peptide receptor (GRPR). The tracer clears rapidly from normal tissues with intense accumulation in the pancreas and excretion occurs via kidneys into the bladder. There is moderate accumulation in the liver and spleen.

J. R. Ballinger, *PET Radiopharmaceuticals*, Clinicians' Guides to Radionuclide Hybrid Imaging, https://doi.org/10.1007/978-3-031-10271-4_31

Activity Administered

130 MBq.

Radiation Dosimetry

Effective dose equivalent (mSv/MBq): 0.091 (11.8 mSv/130 MBq).

Organ doses (mGy/MBq): urinary bladder wall, 1.09; pancreas, 0.23; kidneys, 0.036.

Patient Preparation

No specific preparation required.

Clinical Utility

The gastrin-releasing peptide receptor is overexpressed in a range of cancers where it reflects proliferation. Initial evaluation of RM26 has been in prostate and breast cancer (Cheng et al. 2018; Zhang et al. 2018; Zang et al. 2018; Oroujeni et al. 2019).

Further Reading

Cheng S, Lang L, Wang Z, et al. Positron emission tomography imaging of prostate cancer with Ga-68-labeled gastrin-releasing peptide receptor agonist BBN_{7-14} and antagonist RM26. Bioconjug Chem. 2018;29:410–9.

Oroujeni M, Abouzayed A, Lundmark F, et al. Evaluation of tumor-targeting properties of an antagonistic bombesin analogue RM26 conjugated with a non-residualizing radioiodine label comparison with a radiometal-labelled counterpart. Pharmaceutics. 2019;11:380.

Varasteh Z, Velikyan I, Lindeberg G, et al. Synthesis and characterization of a high-affinity NOTA-conjugated bombesin antagonist for GRPR-targeted tumor imaging. Bioconjug Chem. 2013;24:1144–53.

Zang J, Mao F, Wang H, et al. ^{68}Ga-NOTA-RM26 PET/CT in the evaluation of breast cancer: a pilot prospective study. J Nucl Med. 2018;59(suppl 1):489.

Zhang J, Niu G, Fan X, et al. PET using a GRPR antagonist ^{68}Ga-RM26 in healthy volunteers and prostate cancer patients. J Nucl Med. 2018;59:922–8.

^{68}Ga-FAPI

Contents

Chemical name and alternative names	Chemical structure
DOTA-FAPI FAPI-04 FAPI-4	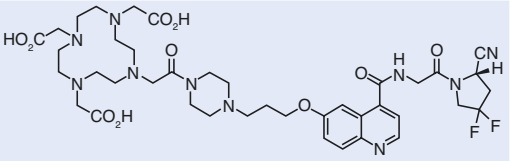

Route of Synthesis

Chelation of generator produced ^{68}Ga-chloride with DOTA-FAPI in acetate buffer at elevated temperature, followed by cartridge purification (Lindner et al. 2018).

Normal Biodistribution and Excretion

FAPI is widely distributed throughout the body and distribution in normal tissues remains relatively constant between 10 min and 3 h post injection. Biodistribution is broadly similar to FDG except for lower activity in the brain, liver, and oral-laryngeal mucosa. Elimination occurs predominantly via the kidneys (Giesel et al. 2019).

Activity Administered

200 MBq.

J. R. Ballinger, *PET Radiopharmaceuticals*, Clinicians' Guides to Radionuclide Hybrid Imaging, https://doi.org/10.1007/978-3-031-10271-4_32

Radiation Dosimetry

Effective dose equivalent (mSv/MBq): 0.016 (3.2 mSv/200 MBq).

Organ doses (mGy/MBq): urinary bladder wall, 0.099; kidneys, 0.044 (Giesel et al. 2019).

Patient Preparation

Not standardized yet.

Clinical Utility

Fibroblast activation protein inhibitors (FAPI) target cancer-associated fibroblasts in a variety of cancers. Thus, FAPI may be an alternative to FDG as a tracer for characterization of tumours (Kratochwil et al. 2019; Chen et al. 2020a, b).

Further Reading

Chen H, Pang Y, Wu J, et al. Comparison of [^{68}Ga]Ga-DOTA-FAPI-04 and [^{18}F] FDG PET/CT for the diagnosis of primary and metastatic lesions in patients with various types of cancer. Eur J Nucl Med Mol Imaging. 2020a;47:1820–32.

Chen H, Zhao L, Ruan D, et al. Usefulness of [^{68}Ga]Ga-DOTA-FAPI-04 PET/CT in patients presenting with inconclusive [^{18}F]FDG PET/CT findings. Eur J Nucl Med Mol Imaging. 2020b; https://doi.org/10.1007/s00259-020-04940-6.

Giesel FL, Kratochwil C, Lindner T, et al. ^{68}Ga-FAPI PET/CT: biodistribution and preliminary dosimetry estimate of 2 DOTA-containing FAP-targeting agents in patients with various cancers. J Nucl Med. 2019;60:386–92.

Kratochwil C, Flechsig P, Lindner T, et al. ^{68}Ga-FAPI PET/CT: tracer uptake in 28 different kinds of cancer. J Nucl Med. 2019;60:801–5.

Lindner T, Loktev A, Altmann A, et al. Development of quinoline-based theranostic ligands for the targeting of fibroblast activation protein. J Nucl Med. 2018;59:1415–22.

Part IV

Oncology—Other Agents

Sodium ^{124}I-Iodide

Contents

Chemical name and alternative names	Chemical structure
None	$Na^{+}\,{}^{124}I^{-}$

Route of Synthesis

Produced in a cyclotron by the ^{124}Te(p,n)^{124}I reaction.

Normal Biodistribution and Excretion

Taken up in thyroid gland by sodium iodide symporter and organified into thyroid hormone. Also accumulates in salivary glands and gastric mucosa. Excreted via the kidneys.

Activity Administered

74 MBq.

Radiation Dosimetry

Effective dose equivalent (mSv/MBq): 0.095 (7 mSv/74 MBq).
Organ doses (mGy/MBq): thyroid, 1.5 at 35% uptake.

J. R. Ballinger, *PET Radiopharmaceuticals*, Clinicians' Guides to Radionuclide Hybrid Imaging, https://doi.org/10.1007/978-3-031-10271-4_33

Patient Preparation

As for other radioiodide studies, iodine-containing medications and foods should be withdrawn to minimise competition by cold iodide for uptake via the sodium iodide symporter. If prior to therapy, uptake should be stimulated by withdrawal of thyroid medications or administration of thyroid-stimulating hormone (rhTSH).

Clinical Utility

Evaluation of patients with differentiated thyroid cancer. Superior image quality and higher sensitivity than ^{131}I planar or SPECT imaging (Phan et al. 2008; Kist et al. 2014; Ruhlmann et al. 2016; Samnick et al. 2018).

Further Reading

Kist JW, de Keizer B, Stokkel MP, et al. Recurrent differentiated thyroid cancer: towards personalized treatment based on evaluation of tumor characteristics with PET (THYROPET study): study protocol of a multicenter observational cohort study. BMC Cancer. 2014;14:405.

Phan HT, Jager PL, Paans AM, et al. The diagnostic value of ^{124}I-PET in patients with differentiated thyroid cancer. Eur J Nucl Med Mol Imaging. 2008;35:958–65.

Ruhlmann M, Jentzen W, Ruhlmann V, et al. High level of agreement between pretherapeutic ^{124}I PET and intratherapeutic ^{131}I imaging in detecting iodine-positive thyroid cancer metastases. J Nucl Med. 2016;57:1339–42.

Samnick S, Al-Momani E, Schmid JS, et al. Initial clinical investigation of [^{18}F]tetrafluoroborate PET/CT in comparison to [^{124}I]iodine PET/CT for imaging thyroid cancer. Clin Nucl Med. 2018;43:162–7.

^{124}I-MIBG

Contents

Chemical name and alternative names	Chemical structure
Meta iodo benzyl guanidine; Iobenguane; mIBG	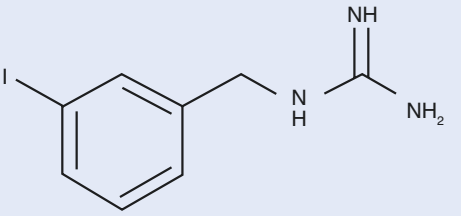

Route of Synthesis

Exchange reaction of ^{124}I-iodide on cold MIBG or electrophilic displacement of a trialkylstannyl precursor.

Normal Biodistribution and Excretion

The uptake of radiolabelled MIBG in different organs depends on catecholamine excretion and/or adrenergic innervation. After intravenous injection, approximately 50% of the administered radioactivity appears in the urine by 24 h, and 70–90% by 48 h. The bladder and urinary tract show intense activity. MIBG is normally taken up mainly by the liver; with lesser uptake in spleen, lungs, salivary glands, skeletal muscles, and myocardium.

Activity Administered

1.0–1.4 MBq/kg, max 50 MBq.

J. R. Ballinger, *PET Radiopharmaceuticals*, Clinicians' Guides to Radionuclide Hybrid Imaging, https://doi.org/10.1007/978-3-031-10271-4_34

Radiation Dosimetry

Effective dose equivalent (mSv/MBq): 0.25 (estimated).

Organ doses (mGy/MBq): thyroid, 2.34; liver, 0.47; urinary bladder wall, 0.46; heart wall, 0.45 (Lee et al. 2010).

Patient Preparation

As with ^{123}I- and ^{131}I-MIBG, a range of drugs must be withdrawn in preparation for a scan.

Clinical Utility

Detection, localisation, staging, and follow-up of neuroendocrine tumours and their metastases. Study of tumour uptake and residence time in order to decide and plan a treatment with high activities of ^{131}I-MIBG (i.e. individual dosimetry). Evaluation of tumour response to therapy by measuring the intensity of MIBG uptake and the.

number of focal MIBG uptake sites. Confirmation of suspected tumours derived from neuroendocrine tissue (Ott et al. 1992; Hartung-Knemeyer et al. 2012; Aboian et al. 2021).

Further Reading

Aboian M, Huang SY, Pampaloni MH, et al. ^{124}I-MIBG PET/CT to monitor metastatic disease in children with relapsed neuroblastoma. J Nucl Med. 2021;62:43–7.

Hartung-Knemeyer V, Rosenbaum-Krumme S, Buchbender C, et al. Malignant pheochromocytoma imaging with [^{124}I]mIBG PET/MR. J Clin Endocrinol Metab. 2012;97:3833–4.

Lee CL, Wahnishe H, Sayre GA, et al. Radiation dose estimation using preclinical imaging with ^{124}I-metaiodobenzyl-guanidine (MIBG) PET. Med Phys. 2010;37:4861–7.

Ott RJ, Tait D, Flower MA, et al. Treatment planning for ^{131}I-mIBG radiotherapy of neural crest tumours using ^{124}I-mIBG positron emission tomography. Br J Radiol. 1992;65:787–91.

^{64}Cu-DOTATATE

Contents

Chemical name and alternative names	Chemical structure
^{64}Cu-N-[(4,7,10-Tricarboxymethyl-1,4,7,10-tetraazacyclododec-1-yl) acetyl]-D-phenylalanyl-L-cysteinyl-L-tyrosyl-D-tryptophanyl-L-lysyl-L-threoninyl-L-cysteinyl-L-threonine-cyclic (2–7) disulphide; Detectnet (curium)	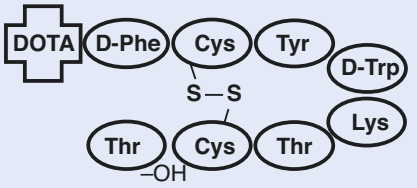

Route of Synthesis

Chelation occurs when ^{64}Cu-chloride is mixed with DOTATATE and ascorbic acid (Pfeifer et al. 2012).

Normal Biodistribution and Excretion

At 1–3 h after intravenous administration, maximum radioactivity is observed in adrenal glands, kidney, pituitary gland, spleen, and liver. There is extensive renal elimination, with 16–40% of the activity recovered in urine over 6 h (Pfeifer et al. 2012).

Activity Administered

148 MBq.

J. R. Ballinger, *PET Radiopharmaceuticals*, Clinicians' Guides to Radionuclide Hybrid Imaging, https://doi.org/10.1007/978-3-031-10271-4_35

Radiation Dosimetry

Effective dose equivalent (mSv/MBq): 0.032 (4.7 mSv/148 MBq).

Organ doses (mGy/MBq): liver, 0.161; kidneys, 0.139; adrenal glands, 0.137; spleen, 0.115 (Pfeifer et al. 2012).

Patient Preparation

Interruption of therapeutic somatostatin analogues with appropriate washout periods.

Clinical Utility

For localisation of somatostatin receptor-positive neuroendocrine tumours (Pfeifer et al. 2015; Johnbeck et al. 2017; Delpassand et al. 2020; Loft et al. 2021).

Further Reading

Delpassand ES, Ranganathan D, Wagh N, et al. ^{64}Cu-DOTATATE PET/CT for imaging patients with known or suspected somatostatin receptor-positive neuroendocrine tumors: results of the first U.S. prospective, reader-masked clinical trial. J Nucl Med. 2020;61:890–6.

Johnbeck CB, Knigge U, Loft A, et al. Head-to-head comparison of ^{64}Cu-DOTATATE and ^{68}Ga-DOTATOC PET/CT: a prospective study of 59 patients with neuroendocrine tumors. J Nucl Med. 2017;58:451–7.

Loft M, Carlsen EA, Johnbeck CB, et al. ^{64}Cu-DOTATATE PET in patients with neuroendocrine neoplasms: prospective, head-to-head comparison of imaging at 1 hour and 3 hours after injection. J Nucl Med. 2021;62:73–80.

Pfeifer A, Knigge U, Binderup T, et al. ^{64}Cu-DOTATATE PET for neuroendocrine tumors: a prospective head-to-head comparison with ^{111}In-DTPA-octreotide in 112 patients. J Nucl Med. 2015;56:847–54.

Pfeifer A, Knigge U, Mortensen J, et al. Clinical PET of neuroendocrine tumors using ^{64}Cu-DOTATATE: first-in-humans study. J Nucl Med. 2012;53:1207–15.

Part V

Cardiology—^{18}F-Labelled Agents

^{18}F-Flurpiridaz

Contents

Chemical name and alternative names	Chemical structure
BMS747158; BMS-747158-02 (Lantheus)	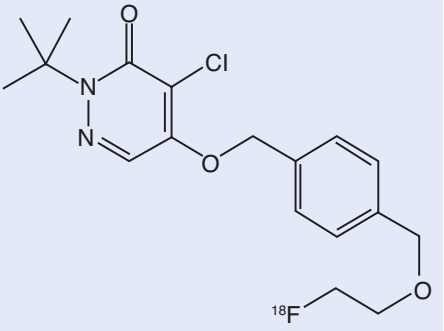

Route of Synthesis

Nucleophilic attack by ^{18}F-fluoride on tosylated precursor followed by HPLC purification and reformulation in saline containing 2% ethanol.

Normal Biodistribution and Excretion

High first pass extraction into cardiomyocytes. Binds to mitochondrial complex I (MCI) found primarily in myocardial cells. Very slow washout from heart. Cleared via kidneys into urine (Maddahi et al. 2011).

J. R. Ballinger, *PET Radiopharmaceuticals*, Clinicians' Guides to Radionuclide Hybrid Imaging, https://doi.org/10.1007/978-3-031-10271-4_36

Activity Administered

100 MBq (rest), 250 MBq (subsequent stress).

Radiation Dosimetry

Effective dose equivalent (mSv/MBq): 0.019 (1.9 + 4.8 mSv/100 + 250 MBq).

Organ doses (mGy/MBq): kidney, 0.066; heart wall, 0.048; liver, 0.039; thyroid, 0.032 (Maddahi et al. 2011).

Patient Preparation

Patients should fast for 4 h. Caffeine-containing products should not be consumed for 12 h. Medications such as beta blockers should be withdrawn.

Clinical Utility

Myocardial perfusion imaging at rest and stress for diagnosis of coronary artery disease (Berman et al. 2013; Packard et al. 2014; Maddahi et al. 2020).

Further Reading

Berman DS, Maddahi J, Tamarappoo BK, et al. Phase II safety and clinical comparison with single-photon emission computed tomography myocardial perfusion imaging for detection of coronary artery disease: flurpiridaz F 18 positron emission tomography. J Am Coll Cardiol. 2013;61:469–77.

Maddahi J, Czernin J, Lazewatsky J, et al. Phase I, first-in-human study of BMS747158, a novel ^{18}F-labeled tracer for myocardial perfusion PET: dosimetry, biodistribution, safety, and imaging characteristics after a single injection at rest. J Nucl Med. 2011;52:1490–8.

Maddahi J, Lazewatsky J, Udelson JE, et al. Phase-III clinical trial of fluorine-18 flurpiridaz positron emission tomography for evaluation of coronary artery disease. J Am Coll Cardiol. 2020;76:391–401.

Packard RR, Huang SC, Dahlbom M, et al. Absolute quantitation of myocardial blood flow in human subjects with or without myocardial ischemia using dynamic flurpiridaz F 18 PET. J Nucl Med. 2014;55:1438–44.

^{18}F-FTPP

Contents

Chemical name and alternative names	Chemical structure
(4-Fluorophenyl)-triphenylphosphonium; BF-PET; Blood-flow PET (FluoroPharma medical)	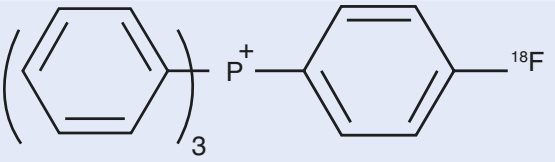

Route of Synthesis

Nucleophilic attack by ^{18}F-fluoride on (4-nitrophenyl)-triphenylphosphonium nitrate followed by HPLC purification and reformulation.

Normal Biodistribution and Excretion

Biodistribution results indicate fast blood clearance, rapid and stable myocardial uptake and high heart to background ratios. Heart activity remained constant over 60 min, while liver activity declined. Organs with highest activity were kidneys, bladder, gall bladder, liver, pancreas, and myocardium.

Activity Administered

74 MBq (rest), 296 MBq (stress).

J. R. Ballinger, *PET Radiopharmaceuticals*, Clinicians' Guides to Radionuclide Hybrid Imaging, https://doi.org/10.1007/978-3-031-10271-4_37

Radiation Dosimetry

Effective dose equivalent (mSv/MBq): 0.018 (1.3 + 5.3 mSv/74 + 296 MBq) (Elmaleh et al. 2009).

Patient Preparation

Patients should fast for 4 h. Caffeine-containing products should not be consumed for 12 h. Medications such as beta blockers should be withdrawn.

Clinical Utility

Myocardial perfusion imaging at stress and rest for diagnosis of coronary artery disease (Shoup et al. 2011).

Further Reading

Elmaleh D, Kardan A, Barrow S, et al. A phase I study evaluating dosimetry and myocardial pharmacokinetic behavior of BFPET, a new F-18 labeled tracer for myocardial perfusion imaging. J Nucl Med. 2009;50(Suppl 2):420.

Shoup TM, Elmaleh DR, Brownell AL, et al. Evaluation of (4-[^{18}F]fluorophenyl)triphenylphosphonium ion. A potential myocardial blood flow agent for PET. Mol Imaging Biol. 2011;13:511–7.

^{18}F-FCPHA

Contents

Chemical name and alternative names	Chemical structure
Trans-9-^{18}F-fluoro-3,4-methylene heptadecanoic acid; ^{18}F-methylene heptadecanoic acid; CardioPET (FluoroPharma medical)	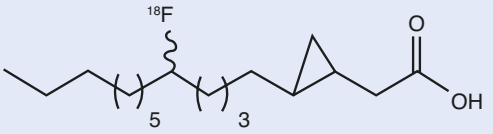

Route of Synthesis

Nucleophilic attack by ^{18}F-fluoride on the mesylate ester precursor, followed by ester hydrolysis, purification, and formulation (Shoup et al. 2005).

Normal Biodistribution and Excretion

Activity clears from the blood pool within 5 min. Activity remains high in liver over 1 h but does not interfere with delineation of myocardium. FCPHA retained in myocardium following metabolism by beta oxidation as a fatty acid analogue (Kardan et al. 2008).

Activity Administered

250 MBq in Phase II trials.

J. R. Ballinger, *PET Radiopharmaceuticals*, Clinicians' Guides to Radionuclide Hybrid Imaging, https://doi.org/10.1007/978-3-031-10271-4_38

Radiation Dosimetry

Effective dose equivalent (mSv/MBq): 0.021 (5.1 mSv/250 MBq).
Organ doses (mGy/MBq): liver, 0.15.

Patient Preparation

Not yet determined.

Clinical Utility

Myocardial perfusion (initial distribution) and fatty acid metabolism (washout) (Demeure et al. 2014, 2015).

Further Reading

Demeure F, Cerqueira M, Gheysens O, et al. FCPHA (CardioPET), a novel F-18 fatty acid analog for myocardial PET imaging: preliminary results of safety, image quality and optimal timing from a phase II trial. Eur J Nucl Med Mol Imaging. 2014;41(suppl 2):S168.

Demeure F, Cerqueira MD, Hesse M, et al. A new F-18 labeled PET tracer for fatty acid imaging. J Nucl Cardiol. 2015;22:391–4.

Kardan A, Shoup T, Barrow S, et al. A phase I study to evaluate the safety and biodistribution of CardioPET as a new cardiac PET tracer: studies in normal subjects. J Nucl Med. 2008;49(Suppl 1):70P.

Shoup TM, Elmaleh DR, Bonab AA, et al. Evaluation of trans-9-^{18}F-fluoro-3,4-methyleneheptadecanoic acid as a PET tracer for myocardial fatty acid imaging. J Nucl Med. 2005;46:297–304.

^{18}F-Flubrobenguane

Contents

Chemical name and alternative names	Chemical structure
1-(3-bromo-4-(3-fluoro-propoxy)benzyl) guanidine; MFBG (Lantheus) LMI1195	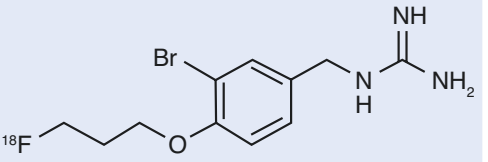

Route of Synthesis

Nucleophilic attack by ^{18}F-fluoride on brosylated precursor followed by HPLC purification and reformulation (Yu et al. 2011).

Normal Biodistribution and Excretion

Activity clears rapidly from the blood and lungs, allowing early cardiac imaging. The tracer undergoes both hepatobiliary and renal excretion. Recovery of activity in the urine accounts for 25% of the dose. Analysis of plasma samples reveals extensive metabolism, with parent drug comprising 37% at 15 min, 13% at 30 min, and 7% at 120 min. LMI1195 is taken into myocardial cells by the norepinephrine transporter (Yu et al. 2011; Sinusas et al. 2014).

Activity Administered

185–370 MBq.

J. R. Ballinger, *PET Radiopharmaceuticals*, Clinicians' Guides to Radionuclide Hybrid Imaging, https://doi.org/10.1007/978-3-031-10271-4_39

Radiation Dosimetry

Effective dose equivalent (mSv/MBq): 0.026 (9.6 mSv/370 MBq).

Organ doses (mGy/MBq): urinary bladder wall, 0.102; kidneys, 0.083; thyroid, 0.066; liver, 0.038 (Sinusas et al. 2014).

Patient Preparation

Not yet determined, but would likely be similar to MIBG, in particular the withdrawal of potentially competing medications.

Clinical Utility

Imaging myocardial sympathetic innervation for risk stratification in heart failure (Yu et al. 2012; Zelt et al. 2019, 2021).

Further Reading

Sinusas AJ, Lazewatsky J, Brunetti J, et al. Biodistribution and radiation dosimetry of LMI1195: first-in-human study of a novel ^{18}F-labeled tracer for imaging myocardial innervation. J Nucl Med. 2014;55:1445–51.

Yu M, Bozek J, Lamoy M, et al. Evaluation of LMI1195, a novel ^{18}F-labeled cardiac neuronal PET imaging agent, in cells and animal models. Circ Cardiovasc Imaging. 2011;4:435–43.

Yu M, Bozek J, Lamoy M, et al. LMI1195 PET imaging in evaluation of regional cardiac sympathetic denervation and its potential role in antiarrhythmic drug treatment. Eur J Nucl Med Mol Imaging. 2012;39:1910–9.

Zelt JG, Britt D, Mair BA, et al. Regional distribution of fluorine-18-flubrobenguane and carbon-11-hydroxyephedrine for cardiac PET imaging of sympathetic innervation. JACC Cardiovasc Imaging. 2021;14:1425–36.

Zelt JG, Mielniczuk LM, Orlandi C, et al. PET imaging of sympathetic innervation with [^{18}F]flubrobenguane vs [^{11}C]mHED in a patient with ischemic cardiomyopathy. J Nucl Cardiol. 2019;26:2151–3.

Part VI

Cardiology—Other Agents

^{11}C-Acetate

Contents

Chemical name and alternative names	Chemical structure
Sodium acetate	CH_3–$^{11}CO_2^-$

Route of Synthesis

Reaction of ^{11}C–CO_2 with methyl magnesium bromide or chloride, followed by hydrolysis and purification.

Normal Biodistribution and Excretion

Taken up in proportion to fatty acid synthesis in most tissues and myocardial perfusion in the heart. Clears from most tissues except pancreas within 20–30 min, allowing visualization of tumours. No urinary excretion.

Activity Administered

740–1480 MBq.

Radiation Dosimetry

Effective dose equivalent (mSv/MBq): 0.0062.

Organ doses (mGy/MBq): pancreas, 0.017; intestines, 0.011; kidneys, 0.0092; spleen, 0.0092.

J. R. Ballinger, *PET Radiopharmaceuticals*, Clinicians' Guides to Radionuclide Hybrid Imaging, https://doi.org/10.1007/978-3-031-10271-4_40

Patient Preparation

No special preparation required.

Clinical Utility

Enzymatic conversion of ^{11}C-acetate to ^{11}C-acetyl-CoA then converted into fatty acids. These are then either incorporated into cellular membranes in proportion to cellular proliferation rate (e.g. in tumours) or oxidised via tricarboxylic acid cycle in normal myocardium. Taken up in prostate cancer and metastases though may also be seen in benign or hyperplastic prostate tissue. Also useful to study fatty acid metabolism in the heart (Armbrecht et al. 1989; Grassi et al. 2012; Nesterov et al. 2015).

Further Reading

Armbrecht JJ, Buxton DB, Brunken RC, et al. Regional myocardial oxygen consumption determined noninvasively in humans with [1-^{11}C]acetate and dynamic positron tomography. Circulation. 1989;80:863–72.

Grassi I, Nanni C, Allegri V, et al. The clinical use of PET with ^{11}C-acetate. Am J Nucl Med Mol Imaging. 2012;2:33–47.

Nesterov SV, Turta O, Han C, et al. C-11 acetate has excellent reproducibility for quantification of myocardial oxidative metabolism. Eur Heart J Cardiovasc Imaging. 2015;16:500–6.

^{13}N-Ammonia

Contents

Chemical name and alternative names	Chemical structure
$^{13}N–NH_3$	$^{13}N–NH_3$

Route of Synthesis

Proton irradiation of natural water (^{16}O) target in cyclotron followed by reduction, distillation, and trapping in a slightly acidic saline solution (Berridge and Landmeier 1993).

Normal Biodistribution and Excretion

Ammonia equilibrates with ammonium ion in the bloodstream. It is the neutral ammonia species which diffuses across biological membranes into cells and is enzymatically converted into glutamine, which is diffusible, or trapped as glutamate. Rapidly cleared from circulation with half-time of 2.8 min, extracted by liver (15%), lungs, myocardium (2–4%), brain, kidney, and bladder. First pass extraction in the heart is 80% at normal flow but falls off at high flow rates. Metabolised in liver through five steps to ^{14}N-urea which appears in the circulation and is excreted via the kidneys.

Activity Administered

740 MBq.

J. R. Ballinger, *PET Radiopharmaceuticals*, Clinicians' Guides to Radionuclide Hybrid Imaging, https://doi.org/10.1007/978-3-031-10271-4_41

Radiation Dosimetry

Effective dose equivalent (mSv/MBq): 0.0022 (1.7 mSv/740 MBq).
Organ doses (mGy/MBq): bladder, 0.007; kidneys, 0.005.

Patient Preparation

Patient should be well hydrated and encouraged to void frequently.

Clinical Utility

Myocardial perfusion imaging at rest and/or stress (Herzog et al. 2009; Fiechter et al. 2012).

Further Reading

Berridge MS, Landmeier BJ. In-target production of [^{13}N]ammonia: target design, products, and operating parameters. Appl Radiat Isot. 1993;44:1433–41.

Fiechter M, Ghadri JR, Gebhard C, et al. Diagnostic value of ^{13}N-ammonia myocardial perfusion PET: added value of myocardial flow reserve. J Nucl Med. 2012;53:1230–4.

Herzog BA, Husmann L, Valenta I, et al. Long-term prognostic value of ^{13}N-ammonia myocardial perfusion positron emission tomography added value of coronary flow reserve. J Am Coll Cardiol. 2009;54:150–6.

^{15}O-Water

Contents

Chemical name and alternative names	Chemical structure
$^{15}O–H_2O$	$^{15}O–H_2O$

Route of Synthesis

A variety of nuclear reactions have been used, including $^{14}N(d,n)^{15}O$, wherein a natural nitrogen target containing 1% oxygen is irradiated with 3–6 MeV deuterons, then hydrogen is added and oxygen is reduced on a platinum or palladium catalyst. Nitrates removed by adsorption on charcoal and soda lime. Alternatively, with the $^{16}O(p,pn)^{15}O$ method, natural water is irradiated with 30 MeV protons, then purified by passage through anion and cation exchange membranes. Can also be inhaled as $^{15}O–CO_2$ which is converted to $^{15}O–H_2O$ in vivo by pulmonary carbonic anhydrase.

Normal Biodistribution and Excretion

Diffuses freely across membranes, entering total body water space. Rapidly diffuses into myocardial cells but also washes out, necessitating subtraction of blood pool activity. Extracted into brain in proportion to regional cerebral perfusion.

Activity Administered

740–2200 MBq.

J. R. Ballinger, *PET Radiopharmaceuticals*, Clinicians' Guides to Radionuclide Hybrid Imaging, https://doi.org/10.1007/978-3-031-10271-4_42

Radiation Dosimetry

Effective dose equivalent (mSv/MBq): 0.0012 (2.6 mSv/2200 MBq).

Organ doses (mGy/MBq): ovaries, 0.0018; lower large intestine, 0.0015; red marrow, 0.0015; upper large intestine, 0.0013 (Brihaye et al., 1995).

Patient Preparation

No special preparation except for medication withdrawal if pharmacological stress is to be used.

Clinical Utility

Myocardial perfusion imaging. Regional cerebral perfusion imaging. Both require processing to produce parametric image (Bergmann et al., 1984; Okazawa et al., 2001).

Further Reading

Bergmann SR, Fox KA, Rand AL, et al. Quantification of regional myocardial blood flow in vivo with $H_2{}^{15}O$. Circulation. 1984;70:724–33.

Brihaye C, Depresseux JC, Comar D. Radiation dosimetry for bolus administration of oxygen-15-water. J Nucl Med. 1995;36:651–6.

Okazawa H, Yamauchi H, Sugimoto K, et al. Quantitative comparison of the bolus and steady-state methods for measurement of cerebral perfusion and oxygen metabolism: positron emission tomography study using ^{15}O-gas and water. J Cereb Blood Flow Metab. 2001;21:793–803.

Rubidium-82

Contents

Chemical name and alternative names	Chemical structure
^{82}Rb rubidium chloride; Cardiogen (Bracco); Ruby-fill (jubilant Draximage)	$Rb^{+}Cl^{-}$

Route of Synthesis

Obtained from chromatographic generator loaded with ^{82}Sr, half-life 25 days.

Normal Biodistribution and Excretion

Following intravenous administration, ^{82}Rb rapidly clears the blood and is extracted by myocardial tissue in a manner analogous to potassium. In human studies, myocardial activity was noted within the first minute after injection. When areas of myocardial infarction are detected with ^{82}Rb, they are visualised within 2–7 min after injection as photon-deficient or "cold areas" on the myocardial scan. Uptake is also observed in kidney, liver, spleen, and lung.

Activity Administered

1480 MBq (1110–2220 MBq).

Assay of ^{82}Sr and ^{85}Sr breakthrough must be performed daily prior to clinical use.

J. R. Ballinger, *PET Radiopharmaceuticals*, Clinicians' Guides to Radionuclide Hybrid Imaging, https://doi.org/10.1007/978-3-031-10271-4_43

Radiation Dosimetry

Effective dose equivalent: 0.95 mSv/2220 MBq.

Organ doses (mGy/2220 MBq): kidney, 19.1; heart, 4.22; lungs, 3.77; small intestine, 3.11.

Patient Preparation

The dose must be administered at a rate of 50 mL/min not to exceed a cumulative volume of 200 mL.

Clinical Utility

Myocardial perfusion imaging (Selwyn et al. 1982; Machac 2005; Renaud et al. 2014; Hagemann et al. 2015; Dilsizian et al. 2016).

Further Reading

Dilsizian V, Bacharach SL, Beanlands RS, et al. ASNC imaging guidelines/SNMMI procedure standard for positron emission tomography (PET) nuclear cardiology procedures. J Nucl Cardiol. 2016;23:1187–226.

Hagemann CE, Ghotbi AA, Kjær A, et al. Quantitative myocardial blood flow with rubidium-82 PET: a clinical perspective. Am J Nucl Med Mol Imaging. 2015;5:457–68.

Machac J. Cardiac positron emission tomography imaging. Semin Nucl Med. 2005;35:17–36.

Renaud JM, Mylonas I, McArdle B, et al. Clinical interpretation standards and quality assurance for the multicenter PET/CT trial rubidium-ARMI. J Nucl Med. 2014;55:58–64.

Selwyn AP, Allan RM, L'Abbate A, et al. Relation between regional myocardial uptake of rubidium-82 and perfusion: absolute reduction of cation uptake in ischemia. Am J Cardiol. 1982;50:112–21.

Part VII

Neurology—^{18}F-Labelled Agents

^{18}F-Florbetapir

Contents

Chemical name and alternative names	Chemical structure
(E)-4-(2-(6-(2-(2-(2-[^{18}F] fluoroethoxy)ethoxy)ethoxy) pyridin-3-yl) vinyl)-*N*-methylaniline; AV-45; Amyvid (Lilly)	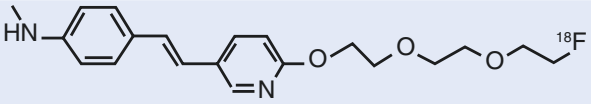

Route of Synthesis

Prepared by nucleophilic substitution of ^{18}F fluoride on tosylate precursor, followed by acid hydrolysis of protecting group. The product is then purified by reversed phase HPLC, trapped, and reformulated with 5% ethanol and ascorbic acid (Yao et al. 2010).

Normal Biodistribution and Excretion

Distributes throughout the body within several minutes, followed by rapid metabolism. Less than 5% of the injected radioactivity remains in the blood after 20 min and less than 2% after 45 min. Maximal brain uptake occurs within several minutes, followed by rapid washout over 30 min. Elimination primarily via the liver and gall bladder into the intestines, but also renal excretion of polar metabolites.

Activity Administered

370 MBq.

J. R. Ballinger, *PET Radiopharmaceuticals*, Clinicians' Guides to Radionuclide Hybrid Imaging, https://doi.org/10.1007/978-3-031-10271-4_44

Radiation Dosimetry

Effective dose equivalent (mSv/MBq): 0.019 (7 mSv/370 MBq).

Organ doses (mGy/MBq): gall bladder wall, 0.143; upper large intestine wall, 0.074; small intestine, 0.066; liver, 0.064 (European Medicines Agency 2013).

Patient Preparation

No special preparation. Use a short intravenous catheter to minimise adsorption and flush with saline to ensure full delivery of the dose. Maximum dilution 1:5 with saline.

Clinical Utility

Imaging of β-amyloid neuritic plaque density in the brains of adult patients with cognitive impairment who are being evaluated for Alzheimer's disease (AD) and other causes of cognitive impairment (European Medicines Agency 2013; Trembath et al. 2015).

Further Reading

European Medicines Agency. Product information: florbetapir (first authorization 2013). 2013. http://www.ema.europa.eu/docs/en_GB/document_library/EPAR_-_Product_Information/human/002422/WC500137635.pdf

Trembath L, Newell M, Devous MD. Technical considerations in brain amyloid PET imaging with ^{18}F-florbetapir. J Nucl Med Technol. 2015;43:175–84.

Yao CH, Lin KJ, Weng CC, et al. GMP-compliant automated synthesis of [^{18}F]AV-45 (Florbetapir F 18) for imaging beta-amyloid plaques in human brain. Appl Radiat Isot. 2010;68:2293–7.

^{18}F-Florbetaben

Contents

Chemical name and alternative names	Chemical structure
4-[(E)-2-(4-{2-[2-(2-[^{18}F] fluoroethoxy)ethoxy]ethoxy} phenyl)-vinyl]-*N*-methylaniline; AV-1; BAY-94-9172; Neuraceq (Piramal)	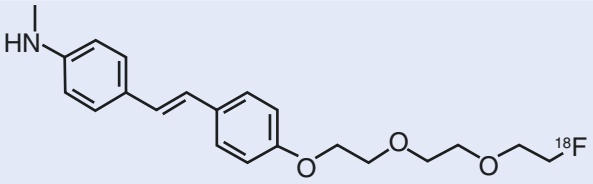

Route of Synthesis

Nucleophilic attack of ^{18}F fluoride on an activated precursor, followed by semi-preparative HPLC purification and reformulation (Wang et al. 2013).

Normal Biodistribution and Excretion

After intravenous bolus injection a radioactivity concentration of 2–3% injected dose/L is achieved in arterial plasma 10 min after injection. Florbetaben is highly bound to plasma proteins (>98.5%). Uptake of radioactivity in the brain is rapid, reaching about 6% of injected radioactivity at 10 min post injection. Florbetaben is eliminated from plasma with a mean biological half-life of about 1 h. No radioactivity could be measured in blood at about 4 h post injection. Based on in vitro investigations, florbetaben is metabolised predominantly by CYP2J2 and CYP4F2. At 12 h post-injection, up to ~30% of the injected radioactivity is excreted with urine.

J. R. Ballinger, *PET Radiopharmaceuticals*, Clinicians' Guides to Radionuclide Hybrid Imaging, https://doi.org/10.1007/978-3-031-10271-4_45

Activity Administered

300 MBq.

Radiation Dosimetry

Effective dose equivalent (mSv/MBq): 0.019 (6 mSv/300 MBq).

Organ doses (mGy/MBq): gall bladder, 0.137; bladder, 0.070; liver, 0.039; upper large intestine, 0.038; lower large intestine, 0.035 (European Medicines Agency 2014).

Patient Preparation

No special preparation. The dose is administered by intravenous slow bolus injection (6 sec/mL) followed by a flush of approximately 10 mL of saline to ensure full delivery of the dose.

Clinical Utility

Florbetaben binds to β-amyloid neuritic plaques in the brain. Healthy controls show relatively low levels of florbetaben retention in cortex. The highest level of uptake is in pons and other white matter regions. In AD subjects, cortical regions and striatal regions show significantly greater uptake compared to controls. In AD subjects, as in controls, there is high retention in pons and other white matter areas. Imaging of β-amyloid neuritic plaque density in the brains of adult patients with cognitive impairment who are being evaluated for Alzheimer's disease (AD) and other causes of cognitive impairment (European Medicines Agency 2014; Becker et al. 2013; Chiaravalloti et al. 2017).

Further Reading

Becker GA, Ichise M, Barthel H, et al. PET quantification of ^{18}F-florbetaben binding to β-amyloid deposits in human brains. J Nucl Med. 2013;54:1–9.

Chiaravalloti A, Danieli R, Lacanfora A, et al. Usefulness of ^{18}F florbetaben in diagnosis of Alzheimer's disease and other types of dementia. Curr Alzheimer Res. 2017;14:154–60.

European Medicines Agency. Product information: florbetaben (first authorization 2014). 2014. http://www.ema.europa.eu/docs/en_GB/document_library/EPAR_-_Product_Information/human/002553/WC500162592.pdf

Wang H, Guo X, Jiang S, et al. Automated synthesis of [^{18}F]florbetaben as Alzheimer's disease imaging agent based on a synthesis module system. Appl Radiat Isot. 2013;71:41–6.

^{18}F-Flutemetamol

Contents

Chemical name and alternative names	Chemical structure
2-[3-[^{18}F]fluoro-4-(methylamino)phenyl]-1,3-benzothiazol-6-ol; 3'-F-PiB; GE-067; AH110690; Vizamyl (GE Healthcare)	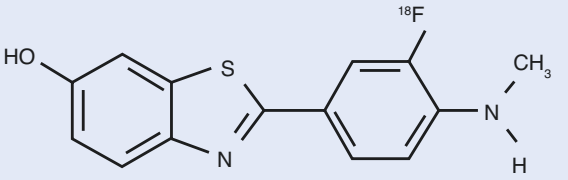

Route of Synthesis

Nucleophilic attack of ^{18}F-fluoride on an activated precursor, followed by cartridge purification and reformulation.

Normal Biodistribution and Excretion

Flutemetamol is distributed throughout the body within several minutes of injection. After 20 min, approximately 20% of the active compound remains in the circulation, falling to 10% at 180 min**.** Maximal flutemetamol brain uptake of approximately 7% of the injected dose occurs within 2 min of administration. This is followed by rapid clearance from the brain in the first 90 min (the recommended time to start scanning), followed by more gradual clearance. Flutemetamol is rapidly cleared from circulation through the intestinal and urinary tracts. At 20 min post-injection, 75% of the radioactivity in plasma was present as polar metabolites, rising to 90% at 180 min. Elimination of flutemetamol is ~37% renal and ~ 52% hepatobiliary. The apparent elimination half-life is 4.5 h.

J. R. Ballinger, *PET Radiopharmaceuticals*, Clinicians' Guides to Radionuclide Hybrid Imaging, https://doi.org/10.1007/978-3-031-10271-4_46

Activity Administered

185 MBq.

Radiation Dosimetry

Effective dose equivalent (mSv/MBq): 0.032 (6 mSv/185 MBq).

Organ doses (mGy/MBq): gallbladder, 0.287; urinary bladder, 0.145; upper large intestine, 0.117; small intestine, 0.102 (European Medicines Agency 2014).

Patient Preparation

No special preparation. The dose is administered by intravenous bolus injection within approximately 40 s. If using an intravenous line, the injection is followed with an intravenous flush of 5–15 mL of saline to ensure full delivery of the dose.

Clinical Utility

PET imaging of β-amyloid neuritic plaque density in the brains of adult patients with cognitive impairment who are being evaluated for Alzheimer's disease (AD) and other causes of cognitive impairment. Flutemetamol should be used in conjunction with a clinical evaluation. A negative scan indicates sparse or no plaques, which is not consistent with a diagnosis of AD (European Medicines Agency 2014; Curtis et al. 2015; Heurling et al. 2016; Martínez et al. 2017).

Further Reading

Curtis C, Gamez JE, Singh U, et al. Phase 3 trial of flutemetamol labeled with radioactive fluorine 18 imaging and neuritic plaque density. JAMA Neurol. 2015;72:287–94.

European Medicines Agency. Product information: flutemetamol (first authorization 2014). 2014. http://www.ema.europa.eu/docs/en_GB/document_library/EPAR_-_Product_Information/human/002557/WC500172950.pdf

Heurling K, Leuzy A, Zimmer ER, et al. Imaging β-amyloid using [^{18}F]flutemetamol positron emission tomography: from dosimetry to clinical diagnosis. Eur J Nucl Med Mol Imaging. 2016;43:362–73.

Martínez G, Vernooij RW, Fuentes Padilla P, et al. ^{18}F PET with flutemetamol for the early diagnosis of Alzheimer's disease dementia and other dementias in people with mild cognitive impairment (MCI). Cochrane Database Syst Rev. 2017;11:CD012884.

^{18}F-Flortaucipir

Contents

Chemical name and Alternative Names	Chemical structure
7-(6-[F-18]fluoropyridin-3-yl)-5H-pyrido[4,3b]indole; AV1451; T807; Tauvid (Lilly)	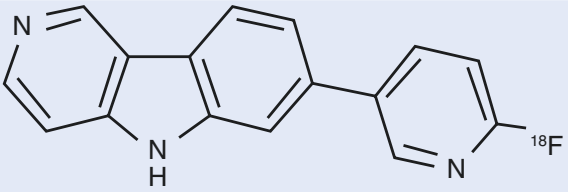

Route of Synthesis

Nucleophilic attack of ^{18}F-fluoride on an N-protected nitro precursor, purified by semi-preparative HPLC followed by reformulation and sterile filtration (Mossine et al., 2017).

Normal Biodistribution and Excrtetion

Flortaucipir binds to aggregated tau protein in neurofibrillary tangles in brain of patients with Alzheimer's disease. Following intravenous injection, flortaucipir is rapidly distributed throughout the body with 10% remaining in the circulation after 5 min and 5% after 10 min. Of the activity remaining in the circulation 80–100 min after injection, 28–34% is the parent drug. Excretion occurs via both hepatobiliary and renal routes.

J. R. Ballinger, *PET Radiopharmaceuticals*, Clinicians' Guides to Radionuclide Hybrid Imaging, https://doi.org/10.1007/978-3-031-10271-4_47

Activity Administered

370 MBq.

Radiation Dosimetry

Effective dose equivalent (mSv/MBq): 0.024 (8.9 mSv/370 MBq).

Organ doses (mGy/MBq): upper large intestine wall, 0.096; small intestine wall, 0.085; liver, 0.057.

Patient Preparation

No special preparation required.

Clinical Utility

Flortaucipir allows estimation of the density and distribution of aggregated intracellular neurofibrillary tangles in the brain of patients with cognitive impairment who are being evaluated for the presence of Alzheimer's disease (Barret et al. 2017; Fleisher et al. 2020).

References

Barret O, Alagille D, Sanabria S, et al. Kinetic modeling of the tau PET tracer ^{18}F-AV-1451 in human healthy volunteers and Alzheimer disease subjects. J Nucl Med. 2017;58:1124–31.

Fleisher AS, Pontecorvo MJ, Devous MD, et al. Positron emission tomography imaging with [^{18}F]flortaucipir and postmortem assessment of Alzheimer disease neuropathologic changes. JAMA Neurol. 2020;77:829–39.

Mossine AV, Brooks AF, Henderson BD, et al. An updated radiosynthesis of [^{18}F]AV1451 for tau PET imaging. EJNMMI Radiopharm Chem. 2017;2:7.

^{18}F-Fallypride

Contents

Chemical name and alternative names	Chemical structure
(S)-*N*-((1-Allyl-2-pyrrolidinyl)methyl)-5-(3-[^{18}F] fluoropropyl)-2,3-dimethoxybenzamide	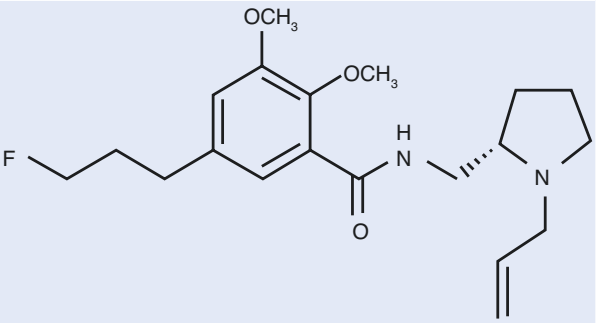

Route of Synthesis

Nucleophilic fluorination of tosyl precursor followed by HPLC purification and reformulation (Mukherjee et al. 1995).

Normal Biodistribution and Excretion

Highest accumulation in muscle, liver, kidneys, and brain. Within the brain, the highest accumulation occurs in the striatum, but significant extra-striatal binding is also observed, particularly in the hypothalamus, thalamus, amygdala, and substantia nigra. At 3 h after injection, 30–40% of the activity in blood is in the form of the parent drug. Excretion occurs via both hepatobiliary and renal routes.

J. R. Ballinger, *PET Radiopharmaceuticals*, Clinicians' Guides to Radionuclide Hybrid Imaging, https://doi.org/10.1007/978-3-031-10271-4_48

Activity Administered

185 MBq.

Radiation Dosimetry

Effective dose equivalent (mSv/MBq): 0.021 (4 mSv/185 MBq).

Organ doses (mGy/MBq): gall bladder wall, 0.12; urinary bladder wall, 0.088; liver, 0.070.

Patient Preparation

No special preparation.

Clinical Utility

Moderate affinity ligand for dopamine D2/3 receptor which demonstrates reversible binding. Useful for studying competition from endogenous dopamine, like ^{11}C-raclopride (Mukherjee et al. 2002; Riccardi et al. 2006, 2008; Dunn et al. 2013).

Further Reading

Dunn JT, Clark-Papasavas C, Marsden P, et al. Establishing test-retest reliability of an adapted [^{18}F]fallypride imaging protocol in older people. J Cereb Blood Flow Metab. 2013;33:1098–103.

Mukherjee J, Christian BT, Dunigan KA, et al. Brain imaging of ^{18}F-fallypride in normal volunteers: blood analysis, distribution, test-retest studies, and preliminary assessment of sensitivity to aging effects on dopamine D-2/D-3 receptors. Synapse. 2002;46:170–88.

Mukherjee J, Yang ZY, Das MK, et al. Fluorinated benzamide neuroleptics--III. Development of (S)-N-[(1-allyl-2-pyrrolidinyl)methyl]-5-(3-[^{18}F]fluoropropyl)-2,3-dimethoxybenzamide as an improved dopamine D-2 receptor tracer. Nucl Med Biol. 1995;22:283–96.

Riccardi P, Baldwin R, Salomon R, et al. Estimation of baseline dopamine D2 receptor occupancy in striatum and extrastriatal regions in humans with positron emission tomography with [^{18}F] fallypride. Biol Psychiatry. 2008;63:241–4.

Riccardi P, Li R, Ansari MS, et al. Amphetamine-induced displacement of [^{18}F] fallypride in striatum and extrastriatal regions in humans. Neuropsychopharmacology. 2006;31:1016–26.

^{18}F-FluoroDOPA

Contents

Chemical name and alternative names	Chemical structure
L-3,4-Dihydroxy-6-[^{18}F]fluoro-phenylalanine; FDOPA	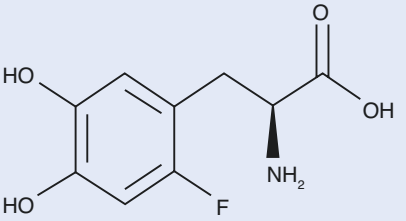

Route of Synthesis

Originally made by electrophilic route by reaction of ^{18}F–F_2 gas with a trialkylstannyl precursor, followed by hydrolysis of protecting groups and purification.

Now it can also be made at high specific activity via nucleophilic route from ^{18}F-fluoride in a multistep procedure (Kuik et al. 2015).

Normal Biodistribution and Excretion

Enters the brain, decarboxylated by ^{18}F-dopamine by the enzyme amino acid decarboxylase and stored in presynaptic nerve terminals in the basal ganglia. Primarily urinary excretion.

Activity Administered

185 MBq.

J. R. Ballinger, *PET Radiopharmaceuticals*, Clinicians' Guides to Radionuclide Hybrid Imaging, https://doi.org/10.1007/978-3-031-10271-4_49

Radiation Dosimetry

Effective dose equivalent (mSv/MBq): 0.026 (4.8 mSv/185 MBq).

Organ doses (mGy/MBq): bladder, 0.215; kidneys, 0.089; pancreas, 0.030 (Harvey et al. 1985; Brown et al. 1998; Kaushik et al. 2013).

Patient Preparation

Fasting for 4 h to reduce competition from other amino acids. Carbidopa (200 mg, 1 h prior to FDOPA), a peripheral decarboxylase inhibitor, may be administered to increase cerebral uptake, suppress physiological uptake in the pancreas, and reduce urinary excretion.

Clinical Utility

Neurology: Study of presynaptic dopaminergic function; differential diagnosis of Parkinson's disease from other neurodegenerative diseases. Measurement of dopamine synthesis rates (Morbelli et al. 2020).

Oncology: As an amino acid analogue for imaging of neuroendocrine tumours and glioma (Evangelista et al. 2019).

Further Reading

Brown WD, Oakes TR, DeJesus OT, et al. Fluorine-18-fluoro-L-DOPA dosimetry with carbidopa pretreatment. J Nucl Med. 1998;39:1884–91.

Evangelista L, Cuppari L, Bellu L, et al. Comparison between ^{18}F-Dopa and ^{18}F-Fet PET/CT in patients with suspicious recurrent high grade glioma: a literature review and our experience. Curr Radiopharm. 2019;12:220–8.

Harvey J, Firnau G, Garnett ES. Estimation of the radiation dose in man due to 6-[^{18}F]fluoro-L-dopa. J Nucl Med. 1985;26:931–5.

Kaushik A, Jaimini A, Tripathi M, et al. Estimation of patient dose in ^{18}F-FDG and ^{18}F-FDOPA PET/CT examinations. J Cancer Res Ther. 2013;9:477–83.

Kuik WJ, Kema IP, Brouwers AH, et al. In vivo biodistribution of no-carrier-added 6-^{18}F-fluoro-3,4-dihydroxy-L-phenylalanine (^{18}F-DOPA), produced by a new nucleophilic substitution approach, compared with carrier-added ^{18}F-DOPA, prepared by conventional electrophilic substitution. J Nucl Med. 2015;56:106–12.

Morbelli S, Esposito G, Arbizu J, et al. EANM practice guideline/SNMMI procedure standard for dopaminergic imaging in parkinsonian syndromes 1.0. Eur J Nucl Med Mol Imaging. 2020;47:1885–912.

^{18}F-FE-PE2I

Contents

Chemical name and alternative names	Chemical structure
[^{18}F]-(*E*)-N-(3-iodoprop-2-enyl)-2β-carbofluoroethoxy-3β-(4′-methyl phenyl) nortropane	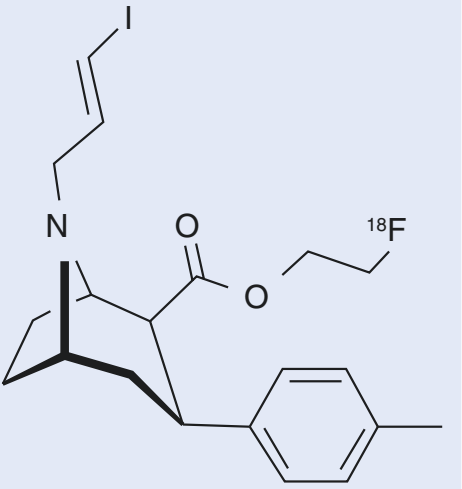

Route of Synthesis

Nucleophilic reaction of ^{18}F-fluoride with a tosylated precursor followed by purification and reformulation (Stepanov et al. 2012).

Normal Biodistribution and Excretion

At early time points (<30 min), activity is the highest in the liver; later (1–6 h) the gall bladder is the highest. Beyond 6 h, only the gall bladder, small intestine, salivary glands, and red marrow show significant activity. The main route of excretion is via the urine (Lizana et al. 2018).

J. R. Ballinger, *PET Radiopharmaceuticals*, Clinicians' Guides to Radionuclide Hybrid Imaging, https://doi.org/10.1007/978-3-031-10271-4_50

Activity Administered

200 MBq.

Radiation Dosimetry

Effective dose equivalent (mSv/MBq): 0.023 (4.6 mSv/200 MBq).

Organ doses (mGy/MBq): urinary bladder, 0.119; liver, 0.046; pancreas, 0.031; kidneys, 0.029 (Lizana et al. 2018).

Patient Preparation

Not standardised yet.

Clinical Utility

Assessment of dopamine transporter function in the striatum of patients with suspected Parkinsonian syndromes (Kerstens et al. 2020; Delva et al. 2020).

Further Reading

Delva A, Van Weehaeghe D, van Aalst J, et al. Quantification and discriminative power of ^{18}F-FE-PE2I PET in patients with Parkinson's disease. Eur J Nucl Med Mol Imaging. 2020;47:1913–26.

Kerstens VS, Fazio P, Sundgren M, et al. Reliability of dopamine transporter PET measurements with [^{18}F]FE-PE2I in patients with Parkinson's disease. EJNMMI Res. 2020;10:95.

Lizana H, Johansson L, Axelsson J, et al. Whole-body biodistribution and dosimetry of the dopamine transporter radioligand ^{18}F-FE-PE2I in human subjects. J Nucl Med. 2018;59:1275–80.

Stepanov V, Krasikova R, Raus L, et al. An efficient one-step radiosynthesis of [^{18}F]FE-PE2I, a PET radioligand for imaging of dopamine transporters. J Labelled Comp Radiopharm. 2012;55:206–10.

^{18}F-FP-DTBZ

Contents

Chemical name and alternative names	Chemical structure
(2R,3R,11bR)-9-(3-^{18}F-fluoropropoxy)-3-isobutyl-10-methoxy-2,3,4,6,7,11b-hexahydro-1H-pyrido[2,1-a]isoquinolin-2-ol; FP-dihydrotetrabenazine; AV-133	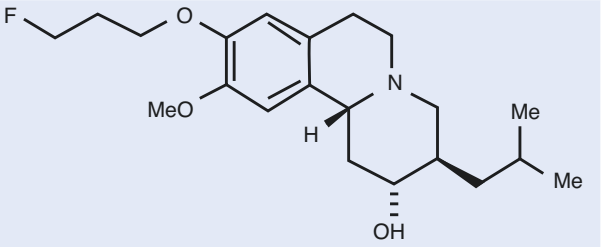

Route of Synthesis

Nucleophilic attack of ^{18}F-fluoride on a tosylated precursor, followed by cartridge purification, reformulation, and membrane filtration (Zhao et al. 2020).

Normal Biodistribution and Excretion

Highest activity is seen in the liver and pancreas, with the intestine appearing at later times. Moderate activity is seen in the kidneys, urinary bladder, bone marrow, and brain. The main route of elimination is hepatobiliary. Within the brain, activity is concentrated in the caudate, putamen, substantia nigra, hippocampus, and brain stem (Lin et al. 2010).

Activity Administered

370 MBq.

J. R. Ballinger, *PET Radiopharmaceuticals*, Clinicians' Guides to Radionuclide Hybrid Imaging, https://doi.org/10.1007/978-3-031-10271-4_51

Radiation Dosimetry

Effective dose equivalent (mSv/MBq): 0.028 (10.4 mSv/370 MBq).

Organ doses (mGy/MBq): pancreas, 0.153; liver, 0.072; upper large intestine, 0.055 (Lin et al. 2010).

Patient Preparation

Not standardised yet.

Clinical Utility

The vesicular monoamine transporter type-2 (VMAT2) is expressed by all monoaminergic neurons and serves to transport neurotransmitter from cytoplasm into vesicles. In the CNS, VMAT2 is expressed exclusively by monoaminergic (dopaminergic, serotonergic, norepinephrinergic, or histaminergic) neurons and > 95% of striatal VMAT2 binding sites are associated with dopaminergic terminals. Thus, VMAT2 is a marker for the early diagnosis of Parkinson's disease and monitoring its progression (Lin et al. 2011, 2013).

Further Reading

Lin KJ, Lin WY, Hsieh CJ, et al. Optimal scanning time window for ^{18}F-FP-(+)-DTBZ (^{18}F-AV-133) summed uptake measurements. Nucl Med Biol. 2011;38:1149–55.

Lin KJ, Weng YH, Hsieh CJ, et al. Brain imaging of vesicular monoamine transporter type 2 in healthy aging subjects by ^{18}F-FP-(+)-DTBZ PET. PLoS One. 2013;8:e75952.

Lin KJ, Weng YH, Wey SP, et al. Whole-body biodistribution and radiation dosimetry of ^{18}F-FP-(+)-DTBZ (18F-AV-133): a novel vesicular monoamine transporter 2 imaging agent. J Nucl Med. 2010;51:1480–5.

Zhao C, Liu C, Tang J, et al. An efficient automated radiosynthesis and bioactivity confirmation of VMAT2 tracer [^{18}F]FP-(+)-DTBZ. Mol Imaging Biol. 2020;22:265–73.

Part VIII

Neurology—^{11}C-Labelled Agents

^{11}C-Raclopride

Contents

Chemical name and alternative names	Chemical structure
S-(2)-3,5-dichloro-*N*-[(1-ethyl-2-pyrrolidinyl)] methyl-2-hydroxy-6-methoxybenzamide	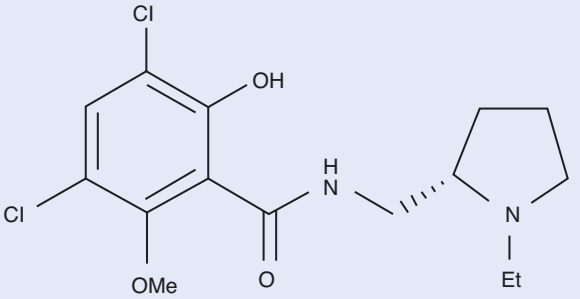

Route of Synthesis

O-methylation of desmethyl precursor with ^{11}C-methyl triflate, followed by HPLC purification and reformulation (Van Laeken et al. 2013).

Normal Biodistribution and Excretion

Activity initially high but clearing rapidly from heart, lung, kidneys, and liver. Activity peaks in gallbladder at 40–60 min. Within the brain, activity highest in basal ganglia (Ribeiro et al. 2005; Slifstein et al. 2006).

Activity Administered

370–555 MBq.

J. R. Ballinger, *PET Radiopharmaceuticals*, Clinicians' Guides to Radionuclide Hybrid Imaging, https://doi.org/10.1007/978-3-031-10271-4_52

Radiation Dosimetry

Effective dose equivalent (mSv/MBq): 0.0087 (4.8 mSv/555 MBq).

Organ doses (mGy/MBq): gallbladder wall, 0.032; small intestine, 0.026; liver, 0.018; urinary bladder wall, 0.014 (Ribeiro et al. 2005; Slifstein et al. 2006).

Patient Preparation

No specific preparation.

Clinical Utility

Reversible binding to dopamine D2/3 receptors in basal ganglia. Sensitive to levels of endogenous dopamine in the synapse. Useful in determination of receptor occupancy of antipsychotic drugs and in studies of addictions (Ginovart 2005; Egerton et al. 2009; Nord and Farde 2011).

Further Reading

Egerton A, Mehta MA, Montgomery AJ, et al. The dopaminergic basis of human behaviors: a review of molecular imaging studies. Neurosci Biobehav Rev. 2009;33:1109–32.

Ginovart N. Imaging the dopamine system with in vivo [^{11}C]raclopride displacement studies: understanding the true mechanism. Mol Imaging Biol. 2005;7:45–52.

Nord M, Farde L. Antipsychotic occupancy of dopamine receptors in schizophrenia. CNS Neurosci Ther. 2011;17:97–103.

Ribeiro MJ, Ricard M, Bourgeois S, et al. Biodistribution and radiation dosimetry of [^{11}C]raclopride in healthy volunteers. Eur J Nucl Med Mol Imaging. 2005;32:952–8.

Slifstein M, Hwang DR, Martinez D, et al. Biodistribution and radiation dosimetry of the dopamine D2 ligand ^{11}C-raclopride determined from human whole-body PET. J Nucl Med. 2006;47:313–9.

Van Laeken N, Kersemans K, De Meestere D, et al. Improved HPLC purification strategy for [^{11}C]raclopride and [^{11}C]DASB leading to high radiochemical yields and more practical high quality radiopharmaceutical formulations. Appl Radiat Isot. 2013;78:62–7.

^{11}C-PiB

Contents

Chemical name and alternative names	Chemical structure
N-methyl-^{11}C-2-(4′-methylaminophenyl)-6-hydroxybenzothiasole; ^{11}C-Pittsburgh compound B; ^{11}C-6-OH-BTA-1	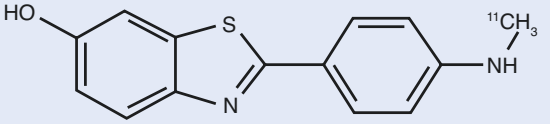

Route of Synthesis

Reaction of ^{11}C-methyl iodide or triflate with the desmethyl precursor, 6-OH-BTA-0, followed by hydrolysis of protecting groups and purification (Mathis et al. 2003).

Normal Biodistribution and Excretion

Rapid entry to and clearance from all cerebral cortical and subcortical grey matter and cerebellum in healthy controls, with relatively lower entry and slower clearance from subcortical white matter. Marked retention in frontal and parietal cortex of patients with Alzheimer's disease in a distribution which post-mortem studies have associated with beta amyloid deposits. Whole body distribution studies show high levels in liver, kidneys, gall bladder, and urinary bladder. Polar metabolites appear in circulation. Unchanged PiB comprises 65–70% at 5 min and 7–10% at 60 min.

Activity Administered

300–500 MBq.

J. R. Ballinger, *PET Radiopharmaceuticals*, Clinicians' Guides to Radionuclide Hybrid Imaging, https://doi.org/10.1007/978-3-031-10271-4_53

Radiation Dosimetry

Effective dose equivalent (mSv/MBq): 0.0053 (2.7 mSv/500 MBq).

Organ doses (mGy/MBq): gallbladder wall, 0.045; urinary bladder wall, 0.026; liver, 0.020; kidneys, 0.013 (O'Keefe et al. 2009).

Patient Preparation

No specific preparation.

Clinical Utility

Binding to beta-amyloid plaques in the brain (Klunk et al. 2004; Mathis et al. 2012).

Further Reading

Klunk WE, Engler H, Nordberg A, et al. Imaging brain amyloid in Alzheimer's disease with Pittsburgh compound-B. Ann Neurol. 2004;55:306–19.

Mathis CA, Mason NS, Lopresti BJ, et al. Development of positron emission tomography β-amyloid plaque imaging agents. Semin Nucl Med. 2012;42:423–32.

Mathis CA, Wang Y, Holt DP, et al. Synthesis and evaluation of ^{11}C-labeled 6-substituted 2-arylbenzothiazoles as amyloid imaging agents. J Med Chem. 2003;46:2740–54.

O'Keefe GJ, Saunder TH, Ng S, et al. Radiation dosimetry of beta-amyloid tracers ^{11}C-PiB and ^{18}F-BAY94-9172. J Nucl Med. 2009;50:309–15.

Part IX

Neurology—^{15}O-Labelled Agents

^{15}O-Water

Contents

Chemical name and alternative names	Chemical structure
$^{15}O–H_2O$	$^{15}O–H_2O$

Route of Synthesis

A variety of nuclear reactions have been used, including $^{14}N(d,n)^{15}O$, wherein a natural nitrogen target containing 1% oxygen is irradiated with 3–6 MeV deuterons, then hydrogen is added and the oxygen is reduced on a platinum or palladium catalyst. Nitrates removed by adsorption on charcoal and soda lime. Alternatively, with the $^{16}O(p,pn)^{15}O$ method, natural water is irradiated with 30 MeV protons, then purified by passage through anion and cation exchange membranes. Can also be inhaled as $^{15}O–CO_2$ which is converted to $^{15}O–H_2O$ in vivo by pulmonary carbonic anhydrase.

Normal Biodistribution and Excretion

Diffuses freely across membranes, entering total body water space. Rapidly diffuses into myocardial cells but also washes out, necessitating subtraction of blood pool activity. Extracted into brain in proportion to regional cerebral perfusion.

Activity Administered

740–2200 MBq.

J. R. Ballinger, *PET Radiopharmaceuticals*, Clinicians' Guides to Radionuclide Hybrid Imaging, https://doi.org/10.1007/978-3-031-10271-4_54

Radiation Dosimetry

Effective dose equivalent (mSv/MBq): 0.0012 (2.6 mSv/2200 MBq).

Organ doses (mGy/MBq): ovaries, 0.0018; lower large intestine, 0.0015; red marrow, 0.0015; upper large intestine, 0.0013 (Brihaye et al. 1995).

Patient Preparation

No special preparation except for medication withdrawal if pharmacological stress is to be used.

Clinical Utility

Myocardial perfusion imaging. Regional cerebral perfusion imaging. Both require processing to produce parametric image (Bergmann et al. 1984; Okazawa et al. 2001).

Further Reading

Bergmann SR, Fox KA, Rand AL, et al. Quantification of regional myocardial blood flow in vivo with $H_2{}^{15}O$. Circulation. 1984;70:724–33.

Brihaye C, Depresseux JC, Comar D. Radiation dosimetry for bolus administration of oxygen-15-water. J Nucl Med. 1995;36:651–6.

Okazawa H, Yamauchi H, Sugimoto K, et al. Quantitative comparison of the bolus and steady-state methods for measurement of cerebral perfusion and oxygen metabolism: positron emission tomography study using ^{15}O-gas and water. J Cereb Blood Flow Metab. 2001;21:793–803.

^{15}O-Oxygen

Contents

Chemical name and alternative names	Chemical structure
$^{15}O–O_2$	$^{15}O–O_2$

Route of Synthesis

Produced using $^{14}N(d,n)^{15}O$ reaction by irradiation of natural nitrogen with 3–6 MeV deuterons.

Normal Biodistribution and Excretion

Administered by inhalation or bolus injection. Inhaled ^{15}O-oxygen is absorbed through the alveoli and binds to haemoglobin. It is carried to all tissues where it is metabolised to ^{15}O-water.

Activity Administered

740 MBq/min.

Radiation Dosimetry

Effective dose equivalent (mSv/MBq): 0.0004.

Organ doses (mGy/MBq): lung, 0.0024; heart, 0.0003; spleen, 0.0002 (Bigler and Sgouros 1983).

J. R. Ballinger, *PET Radiopharmaceuticals*, Clinicians' Guides to Radionuclide Hybrid Imaging, https://doi.org/10.1007/978-3-031-10271-4_55

Patient Preparation

No specific preparation.

Clinical Utility

Measurement of regional cerebral metabolic rate of oxygen ($rCMRO_2$) (Frackowiak et al. 1980; Okazawa et al. 2001; Fan et al. 2020).

Further Reading

Bigler RE, Sgouros G. Biological analysis and dosimetry for ^{15}O-labeled O_2, CO_2, and CO gases administered continuously by inhalation. J Nucl Med. 1983;24:431–7.

Fan AP, An H, Moradi F, et al. Quantification of brain oxygen extraction and metabolism with [^{15}O]-gas PET: a technical review in the era of PET/MRI. NeuroImage. 2020;220:117136.

Frackowiak RS, Lenzi GL, Jones T, et al. Quantitative measurement of regional cerebral blood flow and oxygen metabolism in man using ^{15}O and positron emission tomography: theory, procedure, and normal values. J Comput Assist Tomogr. 1980;4:727–36.

Okazawa H, Yamauchi H, Sugimoto K, et al. Quantitative comparison of the bolus and steady-state methods for measurement of cerebral perfusion and oxygen metabolism: positron emission tomography study using ^{15}O-gas and water. J Cereb Blood Flow Metab. 2001;21:793–803.

^{15}O-Carbon Monoxide

Contents

Chemical name and alternative names	Chemical structure
^{15}O–CO	^{15}O–CO

Route of Synthesis

Produced using ^{14}N(d,n)^{15}O reaction on natural nitrogen with 0.5% oxygen followed by heating with carbon at >1000°C. Nitrogen oxides removed by adsorption with charcoal and soda lime. Essential to maintain high specific activity in order to avoid administering toxic quantities of CO.

Normal Biodistribution and Excretion

Inhaled carbon monoxide binds to haemoglobin in red blood cells, forming carboxyhaemoglobin. Activity remains in blood pool.

Activity Administered

1000 MBq.

By inhalation—single breath hold or continuous.

Radiation Dosimetry

Effective dose equivalent (mSv/MBq): 0.0011.

J. R. Ballinger, *PET Radiopharmaceuticals*, Clinicians' Guides to Radionuclide Hybrid Imaging, https://doi.org/10.1007/978-3-031-10271-4_56

Organ doses (mGy/MBq): lung, 0.0034; heart, 0.0033; spleen, 0.0021 (Bigler and Sgouros 1983).

Patient Preparation

No specific preparation.

Clinical Utility

Regional cerebral blood volume (rCBV) correction in triple oxygen brain studies (Kobayashi et al. 2008).

Further Reading

Bigler RE, Sgouros G. Biological analysis and dosimetry for ^{15}O-labeled O_2, CO_2, and CO gases administered continuously by inhalation. J Nucl Med. 1983;24:431–7.

Kobayashi M, Kudo T, Tsujikawa T, et al. Shorter examination method for the diagnosis of misery perfusion with count-based oxygen extraction fraction elevation in ^{15}O-gas PET. J Nucl Med. 2008;49:242–6.

^{15}O-Carbon Dioxide

Contents

Chemical name and alternative names	Chemical structure
$^{15}O–CO_2$	$^{15}O–CO_2$

Route of Synthesis

Produced using $^{14}N(d,n)^{15}O$ reaction on natural nitrogen with 4% oxygen followed by heating with activated charcoal at 600 °C.

Normal Biodistribution and Excretion

Inhaled ^{15}O-carbon dioxide diffuses across the alveolar membrane and is converted to ^{15}O-water in capillary blood. It then enters the total body water space. This includes crossing the blood–brain barrier as a marker of regional cerebral blood flow.

Activity Administered

1000 MBq.

By inhalation—single breath hold or continuous.

Radiation Dosimetry

Effective dose equivalent (mSv/MBq): 0.00054.

Organ doses (mGy/MBq): lung, 0.0012; adrenals, 0.00049; breast, 0.00048 (Bigler and Sgouros 1983; Meyer et al. 1987).

J. R. Ballinger, *PET Radiopharmaceuticals*, Clinicians' Guides to Radionuclide Hybrid Imaging, https://doi.org/10.1007/978-3-031-10271-4_57

Patient Preparation

No specific preparation.

Clinical Utility

Measurement of regional cerebral blood flow (rCBF) (Ibaraki et al. 2008).

Further Reading

Bigler RE, Sgouros G. Biological analysis and dosimetry for ^{15}O-labeled O_2, CO_2, and CO gases administered continuously by inhalation. J Nucl Med. 1983;24:431–7.

Ibaraki M, Miura S, Shimosegawa E, et al. Quantification of cerebral blood flow and oxygen metabolism with 3-dimensional PET and ^{15}O: validation by comparison with 2-dimensional PET. J Nucl Med. 2008;49:50–9.

Meyer E, Yamamoto LY, Evans AC, et al. Radiation dose to upper airways from inhaled oxygen-15 carbon dioxide. J Nucl Med. 1987;28:234–9.